Preface

The *Space Programs Summary* is a six-volume, bimonthly publication that documents the current project activities and supporting research and advanced development efforts conducted or managed by JPL for the NASA space exploration programs. The titles of all volumes of the *Space Programs Summary* are:

Vol. I. The Lunar Program (Confidential)

Vol. II. The Planetary–Interplanetary Program (Confidential)

Vol. III. The Deep Space Network (Unclassified)

Vol. IV. Supporting Research and Advanced Development (Unclassified)

Vol. V. Supporting Research and Advanced Development (Confidential)

Vol. VI. Space Exploration Programs and Space Sciences (Unclassified)

The *Space Programs Summary,* Vol. VI consists of an unclassified digest of appropriate material from Vols. I, II, and III; an original presentation of technical supporting activities, including engineering development of environmental-test facilities, and quality assurance and reliability; and a reprint of the space science instrumentation studies of Vols. I and II.

W. H. Pickering, *Director*
Jet Propulsion Laboratory

Space Programs Summary No. 37-33, Volume II

Copyright © 1965, Jet Propulsion Laboratory, California Institute of Technology

Prepared under Contract No. NAS 7-100, National Aeronautics & Space Administration

[redacted] contains information affecting the nati[redacted]efense of the United States, within the mean[redacted]aws, Title 18, U.S.C., Sections 793 and 794, the tra[redacted]ion or revelation of which in any manner to an unauthori[redacted]erson is prohibited by law.

UNCLASSIFIED

Contents

I. *Mariner* Mars 1964 Project 1
A. Introduction 1
B. Project Engineering 2
C. Systems 3
D. Guidance and Control 4
E. Spacecraft Design 11

II. *Voyager* Project 15
A. Introduction 15
B. Advanced Operational Support Equipment Development for Central Computer and Sequencer 16

III. Future Projects 22
A. Asteroid Belt and Jupiter Flyby Mission Study 22
B. Variable Orbit Mars Atmospheric Probe 41

UNCLASSIFIED

[redacted] UNCLASSIFIED

I. *Mariner* Mars 1964 Project

A. Introduction

The early objective of the Planetary-Interplanetary Program is the initial probing of the planets Mars and Venus by unmanned spacecraft. The initial probing of Venus was successfully accomplished by *Mariner II*. The next step toward this objective was the initial probing of Mars by the *Mariner IV* spacecraft, which is now in transit.

The primary objective of the *Mariner C* mission (*Mariner* Mars 1964 Project) is to conduct close-up (flyby) scientific observations of the planet Mars during the 1964–1965 opportunity and to transmit the results of these observations back to Earth. The planetary observations should, to the greatest practical extent, provide maximum information about Mars. TV, cosmic dust, and a reasonable complement of fields and particles experiments are being carried. In addition, an Earth occultation experiment is planned to obtain data relating to the scale height and pressure in the atmosphere of Mars.

A secondary objective is to provide experience and knowledge about the performance of the basic engineering equipment of an attitude-stabilized flyby spacecraft during flight in space farther away from the Sun than the Earth. An additional objective is to perform certain field and/or particle measurements in interplanetary space during the trip and in the vicinity of Mars.

The *Mariner III (MC-2)* spacecraft was launched on November 5, 1964. The nose cone failed to eject from the spacecraft, thereby precluding solar panel deployment; the battery power was depleted 8 hr and 43 min after launch.

The *Mariner IV (MC-3)* spacecraft was successfully injected into a Mars encounter orbit about the Sun on November 28, 1964. All subsystems are performing as designed, with two exceptions: the solar plasma probe is degraded due to a power supply failure (discussed in previous *SPSs*), and the ion chamber experiment has failed.

On March 5, 1965 the central computer and sequencer (CC&S) switched the spacecraft transmitter from the low- to the high-gain antenna, as planned. *Mariner IV* continues to receive on the low-gain antenna. All communications system performance has been within tolerance and has functioned without incident during this period.

UNCLASSIFIED [redacted]

The DSIF Station 51 at Johannesburg was released to the *Ranger* Project for the period March 11 to 26, resulting in a loss of about 7 hr/day of telemetry from *Mariner IV*.

The ion chamber failure occurred on March 17 while the spacecraft was over Johannesburg. The failure has been duplicated in the laboratory at Massachusetts Institute of Technology, and results indicate that the failures of the Geiger-Mueller 10311 tube and the ion chamber both occurred within a common power supply. There have been no detectable effects on the remainder of the spacecraft to date as a result of these failures.

On April 2 the CC&S commanded the second updating of the Canopus tracker cone angle. This event occurred without incident. Two more steps of this cone angle are planned before encounter.

By April 30 *Mariner IV* was in flight for 153 days, surpassing the *Mariner II* record of 129 days. At the same date, the communication distance (Earth to probe) was 67.4 million miles, surpassing all known distance records.

The cosmic dust or micrometeorite impacts upon the cosmic dust detector have shown a marked increase during this period. The average rate has risen from one to two hits per week shortly after launch to about three per day and is expected to increase. By comparing the area of the cosmic dust detector to that of the entire spacecraft, it is computed that for each hit on the detector there are 200 hits on the spacecraft. No detectable effect from these events has been seen to date on any spacecraft subsystem.

The *MC-4* spacecraft (flight spare) and its associated operational support equipment have been returned to JPL for bonded storage. The spacecraft will be subjected to a complete system test before going into controlled storage. The storage specifications are based on a 2-yr period. A study of potential uses for the *MC-4* spacecraft was made. Many different purposes or missions were investigated, but the one considered to be the most valuable was another Mars mission at the next launch opportunity in 1966. No definite action has been taken this time regarding this proposal.

A magnetics workship was held at JPL from March 30 to April 1. The program is described in Sect. B of this issue.

A thermal control workshop will be held in June of this year. The intent is to provide an opportunity for comparison of experience in several NASA flight projects regarding thermal control techniques and effectiveness.

B. Project Engineering

1. Environmental Requirements

a. Magnetics workshop

Background. The successful demagnetizing of the *Mariner* solar panels in the Earth's field at Cape Kennedy during October 1964 stimulated increased interest in spacecraft magnetic cleanliness. A magnetics workshop was conducted at JPL on March 30, 31 and April 1, 1965 to exchange technical information and provide documentation of NASA's experience in developing magnetically clean spacecraft. Dr. E. A. Gaugler, of NASA Headquarters, was chairman of the workshop. A large cross-section of organizations involved in spacecraft low magnetic field efforts attended, representing thirty-five industrial concerns, seven universities, six NASA centers or offices, two Navy agencies and an Air Force activity.

Technical Program. The following formal presentations were made at the sessions listed. Talks were followed by open discussion periods of about 30 min.

SESSION ON EXPERIMENTERS' PROBLEMS WITH MAGNETIC SPACECRAFT AND MAGNETOMETER LOCATIONS

"Recommendations of the Particles and Fields Subcommittee and the Importance of Interplanetary Magnetic Field Measurements," Dr. C. P. Sonett, Ames Research Center, Moffett Field, Calif.

"Problems of Magnetic Contamination," Dr. Edward J. Smith, Jr., Jet Propulsion Laboratory, Pasadena, Calif.

"Remarks on the Need for Interplanetary Magnetic Field Measurements," Prof. L. Davis, Jr., California Institute of Technology, Pasadena, Calif.

SESSION ON DESIGN CONSIDERATIONS FOR A MAGNETICALLY CLEAN SPACECRAFT

"Competing Spacecraft Design Characteristics," J. R. Casani, Jet Propulsion Laboratory, Pasadena, Calif.

"Establishment of Spacecraft Magnetic Criteria and Design Restraints," J. E. Maclay, Jet Propulsion Laboratory, Pasadena, Calif.

"Magnetic Program for *Pioneer* and Its Scientific Payload," E. J. Iufer, Ames Research Center, Moffett Field, Calif.

SESSION ON SPACECRAFT FIELD PREDICTION AND MEASUREMENT

"Magnetic Testing of Spacecraft," L. C. Parsons, Goddard Space Flight Center, Greenbelt, Md.

"*Mariner* Mars Magnetic Mapping Tests," Dr. J. A. Stallkamp, Jet Propulsion Laboratory, Pasadena, Calif.

"A Resonance Technique for Measurement of Satellite Magnetic Dipole Moment," Barry E. Tossman, Applied Physics Laboratory, Johns Hopkins University, Silver Spring, Md.

SESSION ON MAGNETIC TEST FACILITIES

"Development of Magnetic Test Facilities at Goddard Space Flight Center," W. G. Brown, Goddard Space Flight Center, Greenbelt, Md.

"Room-size Magnetic Shield Facility," B. V. Connor, Jet Propulsion Laboratory, Pasadena, Calif.

"Magnetic Mapping of *Mariner* Mars Assemblies," A. M. A. Frandsen, Jet Propulsion Laboratory, Pasadena, Calif.

"Magnetic Test Facilities at Ames Research Center and Malibu," E. J. Iufer, Ames Research Center, Moffett Field, Calif.

"A Stable Field Environment for Magnetometer Testing," Dr. R. E. Brown, U. S. Naval Ordnance Laboratory, Silver Spring, Md.

"Biological Aspects of a Zero Magnetic Field Environment," Dr. D. E. Beischer, Naval School of Aviation Medicine, Pensacola, Fla.

SESSION ON DEPERMING AND MAGNETIC SHIELDING

"Design of Spacecraft Demagnetizing Coils," A. M. A. Frandsen, Jet Propulsion Laboratory, Pasadena, Calif.

"Solar Panel Deperming," J. G. Bastow, Jr., Jet Propulsion Laboratory, Pasadena, Calif.

"On the Magnetic Shielding of Spacecraft Hardware," J. Robert Christy, Jet Propulsion Laboratory, Pasadena, Calif.

"Magnetic Shielding Experiences," D. D. Norris, Jet Propulsion Laboratory, Pasadena, Calif.

"Deperming of OGO," Dr. J. W. Lindner, TRW-Space Technology Laboratories, Inc., Redondo Beach, Calif.

SESSION ON PREFERRED MATERIALS AND PARTS

"Metallic Materials for Non-Magnetic Spacecraft – Properties and Measurement Methods," R. H. Lundsten and D. I. Gordon, Naval Ordnance Laboratory, Silver Spring, Md.

"Magnetic Classification of Metallic Materials for Spacecraft Usage," J. Robert Christy, Jet Propulsion Laboratory, Pasadena, Calif.

"Non-Magnetic High Reliability Components?," Howard Friedman, Jet Propulsion Laboratory, Pasadena, Calif.

"The Unique Non-Magnetic Nitinol Alloys," William J. Buehler, U. S. Naval Ordnance Laboratory, Silver Spring, Md.

"Preferred Parts and Materials," E. J. Iufer, Ames Research Center, Moffett Field, Calif.

"A Microgaussmeter," Alex Grumet, Republic Aviation Corp., Farmingdale, N. Y.

Conclusions. The workshop highlighted the fact that it takes a constant awareness of the fundamentals of magnetism on the part of every designer and a real interest on the part of management to produce a magnetically clean spacecraft. Although magnetic specifications generally deal with the end product, the techniques and steps necessary for meeting these specifications must be taken very early in the design phases of the project. Subsequent efforts can only lead to increased cost and less stable or thorough results. A second important concept expressed was that magnetic testing of subassemblies should be frequent and should be followed by positive corrective action. In the area of materials, there appears to be a wide range of nonmagnetic materials available, and an increasing number of nonmagnetic electronic components are becoming available when specifically requested. An important and widespread application which still resists solution is the availability of an entirely satisfactory nonmagnetic glass to metal seal.

The complete proceedings including discussions and comments is now being compiled and will be published in limited quantity as Technical Memorandum 33-216 on approximately July 1 for distribution to the various attendees. A few additional JPL copies will be available for distribution as authorized by NASA Headquarters.

C. Systems

1. Space Flight Operations

Space flight operations (SFO) activities, covering the report period March and April 1965, have been directed toward the planning, coordination and participation in three encounter tests (using the *Mariner* proof-test model), flight operations for *Mariner IV*, and the generation of *Mariner IV* Progress Reports and daily Technical Bulletins.

a. Flight operations for Mariner IV. Spacecraft performance during the period was nominal, and the following standard (planned) events were executed:

(1) CC&S command MT-5 was issued on March 5 at 13:02:40 GMT. MT-5 switched the spacecraft transmitter to the high-gain antenna.

(2) CC&S command MT-2 was issued on April 2 at 14:25:15 GMT. MT-2 changed the Canopus cone angle from No. 1 to No. 2 set.

The following nonstandard events occurred:

(1) Disturbances in the roll channel of the attitude-control system were observed on March 11, 14, 18 and April 7, 11, 15, and 24. No loss of Canopus intensity was observed.

(2) The Geiger-Mueller 10311 tube, associated with the ion chamber, was declared inoperative.

(3) Fluctuations in the ground-received signal strength were observed that were apparently due to interference patterns between the high- and low-gain antennas.

(4) Sudden drops in received signal strength coincident with the CC&S cyclic pulses were observed by the DSIF while in one-way lock.

(5) The spacecraft battery voltage continued to rise even though the battery charger was off. This is believed due to a slight trickle charge from the battery voltage transducer and unexpected sensitivity to small charge currents at a battery temperature between 60 and 70°F. It is not expected to rise above 35.7 v, although the upper limit is presently 36.0 v.

(6) The ion chamber experiment failed on March 17 during the Johannesburg Tracking Station (DSIF 51) view period. No telemetry data were being received from the spacecraft at the time of the failure, as DSIF 51 was assigned to the *Ranger* Project and was not tracking *Mariner IV*.

(7) A 1-db decrease in average ground-received carrier power approximately coincident with the MT-2 command on April 2.

A number of milestones were reached during this period. The major one occurring on April 14 at 09:41 GMT when *Mariner IV* spacecraft exceeded the DSIF communications distance record of 86.677 million kilometers set by *Mariner II* in January 1963.

D. Guidance and Control

1. Spacecraft Power System

a. Mariner IV flight analysis. Operation of the *Mariner IV* power system continues to be satisfactory after 153 days of flight. The only item that is presently causing some concern is the slowly increasing battery voltage. This increase is due primarily to the small 1- to 2-ma charging current from the battery telemetry voltage transducer plus the decreasing battery temperature. If the rate of increase remains constant, the battery voltage will be approximately 37.0 v dc at encounter. This would mean an average cell voltage of 2.05 v, approaching a voltage (and hence an internal pressure) at which battery leakage becomes more likely. A life-test battery is being used to simulate the condition of the *Mariner IV* battery. It is being operated at a lower temperature and a slightly higher voltage than the flight battery, in an attempt to predict future operation of the *Mariner IV* unit. The test will continue until Mars encounter.

The solar panels continue to operate normally. Solar panel power predictions, made shortly before launch and based on a known trajectory and an anticipated temperature profile, continue to be an accurate representation of panel performance (*SPS 37-32*). The closeness of the original prediction and the present performance is based on four items:

(1) The trajectory, and hence the solar intensity, was known with good accuracy at the time the predictions were made.

(2) Actual solar panel temperatures agree closely with those used in the power predictions.

(3) The solar panel standard cells agree reasonably well with the predicted panel power, and no radiation degradation has been observed.

(4) The solar panel operating point, voltage and currents, leads to a combined I versus V curve that gives a maximum power point consistent with the power predictions.

On April 1 the decreasing solar panel zener diode voltage intersected the increasing solar panel operating point voltage. Both voltage variations are due to decreasing solar panel temperature. The result was a 1-DN 0.2-v shift in the operating point voltage. As the solar panels continue to cool, a slowly varying electrical-thermal equilibrium between the panel sections and the zeners will be established. This may result in minor changes in

the solar panel operating point, voltage and currents, but these changes will have no effect on power subsystem performance and will not affect the maximum power capability of the panels.

2. Attitude-Control Subsystem: Flight Performance from Launch to April 1, 1965

a. Initial Sun acquisition. The first function performed by the *Mariner IV* spacecraft was the reduction of the separation rates generated by the process of separation from the *Agena* booster. The spacecraft was injected into orbit while in the Earth's shadow, and the only attitude-control information was rate information about each controlled axis obtained from rate gyros. These rate gyros furnish rate feedback into switching amplifiers that activate gas jets utilizing cold nitrogen to produce clockwise and counterclockwise torques about each axis for control purposes. The switching amplifiers have a built-in deadband, so that if the input is less than a given amount, no gas valve actuation occurs. For signals greater than the deadband, the gas jets are switched on to provide constant control torques to null out the error signals into the switching amplifiers. Normally, position information from a Sun sensor is also employed to furnish rate plus position information for control. Since the spacecraft was injected into orbit in the Earth's shadow, only gyro rate information was available, and the rate feedback reduced the rates to the deadband values. These were ± 1.27 mrad[1]/sec in pitch and yaw and ± 0.33 mrad/sec in roll. When the spacecraft was first observed in the shadow, the rates were already within the deadband, indicating that the separation rates were very low.

When the spacecraft emerged into the sunlight, Sun sensors which provide 360 deg field-of-view information about both the pitch and yaw axes, provided additional attitude-control information to reduce the position errors to the switching amplifier deadband values. These values are ± 8.6 mrad. These sensors have saturated outputs at about $\pm 11.^{\circ}5$, and beyond that value the rate plus position information is a constant input to drive the spacecraft at a constant rate toward null. When the position signals come out of saturation, the proportional position signals reduce the position error to the deadband value.

The actual time of exit from the Earth's shadow took place at 333:15:17:35 GMT[2] but Sun sensor signals were first noted at 15:16:37 GMT due to the refraction of sunlight through the Earth's atmosphere.

When the spacecraft was fully in the sunlight the pitch error was seen to be equal to $-1.^{\circ}0$, and for all practical purposes the pitch axis had acquired. The yaw Sun sensors were saturated and had established a rate determined by this saturation equal to -2.2 mrad/sec (-0.126 deg/sec). The yaw sensors came out of saturation at 15:29:56 GMT at an angle of $+11.^{\circ}5$. This would indicate that at the start of yaw acquisition, the yaw angle was about $+106$ deg.

After initial Sun acquisition has occurred, the spacecraft roll axis is pointed at the Sun, but at that point, there is only gyro rate control about the roll axis. One of the functions of the attitude-control system was to provide a constant roll rate about the roll axis so that it would be possible to calibrate the science magnetometer. This was accomplished by an on-board logic system employing a small Sun sensor with a cone angle field-of-view, about the roll axis, of about 2 deg. When the spacecraft has acquired the Sun in pitch and yaw and the cone angle Sun sensor is illuminated, a constant voltage is automatically applied to the roll switching amplifier and the rate feedback causes the spacecraft to spin about the roll axis at a constant rate. This logic system is called the Sun gate.

A Sun gate event occurred at 15:30:59 GMT. This indicates that the Sun gate cone angle field-of-view was $2.^{\circ}2$, which is within the design tolerance.

The Sun gate initiated the magnetometer calibration spin as required. A search signal was switched into the roll-axis control system and the spacecraft accelerated to a rate of -3.55 mrad/sec (-0.203 deg/sec), which is the design nominal.

During the magnetometer spin mode, the pitch and yaw errors were observed to limit cycle against one side of the deadband. The pitch axis stayed at $+8.7$ mrad edge and yaw at the -8.5 mrad edge. This is as expected and is due to cross-coupling from the cross-products of inertia.

b. Roll control. After the period of magnetometer calibration, it is necessary to establish three-axis attitude control. This is accomplished by using a star tracker to lock onto the star Canopus, which is used as a roll-angle reference. The star tracker has a total field-of-view of about 5 deg about the roll axis (clock angle) and 10 deg

[1] mrad = milliradian

[2] Day of year: hr: min: sec.

perpendicular to the roll axis (cone angle). At 66⅔ hr after launch, the central computer and sequencer (CC&S) switches the roll-control system from magnetometer calibrate to Canopus acquisition mode. A smaller signal is switched into the roll-switching amplifier to furnish a smaller search rate suitable for star acquisition. On-board logic is provided using star brightness and roll error signals to diminish the number of possible celestial objects that might activate the star tracker. If an object is less than ¼ or greater than 8 times brighter than Canopus, the automatic search is continued. If an object falls within that range, with a negative 4.0-v position error signal, the search signal is switched out and acquisition takes place. Unfortunately, there are still many acquirable objects, and if the wrong object is acquired, a ground command, roll override (DC-21) may be sent to initiate a new roll search. The problem still remains to properly identify any object that is acquired. This is discussed below.

After a star has been acquired, all the gyros are switched off to conserve power and a passive stabilization system is used for the cruise mode of operation. The gyros are shut down after a 200-sec time delay from the time the acquisition logic circuitry is activated. The passive stabilization is called "derived rate," and consists of a lag feedback with a long time constant around each switching amplifier. Whenever the gas jets are fired, the long time constant lag output looks like a rate feedback signal and is fed into the switching amplifier input for stabilization. If the spacecraft rates are low, as in the cruise mode, this acts very much like the real rate feedback. If the star or Sun acquisition is ever lost, the gyros go on automatically due to the acquisition logic, the Sun will be acquired, and the Sun gate will institute a roll search for a star. In the event that only the star is lost, an automatic roll search is instituted.

Star identification procedure. Before the spaceflight it was felt that star identification would be a major problem. This was derived from the fact that the only information from the star tracker, other than an error signal, is a brightness measurement and the cone angle of an object within ± 5 deg. The absolute calibration of the star tracker for all the stars in the sky is not known, and the problem is further complicated by the brightness signal including the integrated background of stars in the field. But during the roll search mode the tracker makes good relative measurements of the star plus background brightness. This information is basic to the star identification procedure.

A map-matching technique was developed to identify objects seen by the star tracker during the roll-search mode. As an aid to establishing the map-matching technique, other corroborating information was used for initial acquisition. These included a fixed wide angle (26×83 deg) field-of-view Earth detector, to provide an output if Canopus were in the star tracker; magnetometer information obtained during the calibration mode for rate and position information; and low-gain antenna pattern variations also to provide rate and position information. The magnetometer and antenna information is very crude and could be used only with a low weighting function on their corroboration.

Fundamental to the map matching was an *a priori* telemetry map of tracker brightness output versus clock angle (angle about the Sun line measured from Canopus). A reasonably sophisticated mathematical model of the star tracker and the sky, including the Milky Way, was developed so that, with the trajectory information, a 7094 program printed a map of the expected telemetry output of the brightness channel seen during roll search. This then would be matched with an actual telemetry map to identify observed objects.

Initially, an extensive computer program was devised to process the telemetry data to produce the actual telemetry map. This was statistically correlated with the *a priori* map, Earth detector output, magnetometer data, and low-gain antenna data. Whenever an object was acquired subsequent to a roll search, a calculation was made of the probability that each acquirable object had been acquired. If the object were not Canopus, roll override would institute another roll search and another computer run was made until Canopus was identified as acquired.

The computer-generated version of the map matching was necessary, due to the lack of knowledge of the tracker response to innumerable objects and integrated background that would be seen by the tracker. Until the tracker could actually be calibrated in flight, the uncertainties required that the best possible analysis techniques be prepared beforehand.

In addition to the computer-generated star identification program, a second map-matching technique was developed and implemented during the flight, which was much simpler, but required actual flight experience to prove reliability. A continuous strip chart recorder

was employed to plot in real-time the star tracker brightness telemetry. An *a priori* map, derived from the computer program was transcribed to a transparent overlay to the same scale as the real-time telemetry plot, so that they could be instantaneously compared during the roll search. The process turned out to be surprisingly good and became the primary technique for star identification. It was quite accurate and the fastest possible way of identifying objects. One of the mission accomplishments can be said to be the development of the procedure consisting of excellent *a priori* maps matched in real-time with brightness telemetry data.

First star acquisition. Initial roll acquisition was commanded by the CC&S to take place at 334:06:59:00 GMT. Just prior to this command (CC&S L-3), the spacecraft was in the magnetometer calibration mode, rolling at a rate of −3.55 mrad/sec (−0.203 deg/sec). At the roll acquisition command, the search command signal was switched in, and the roll rate was reduced to −2.35 mrad/sec (−0.135 deg/sec) which, as would be expected, is the upper edge of the deadband about the nominal search rate. An acquisition occurred at 7:7:47 GMT. At this point, Earth light reflections on the star tracker optics caused a bright enough background, along with a spurious error signal, to cause the acquisition logic to discontinue the roll search. Even though there was no acquirable object, a logic acquisition had been effected. The clock angle at this point was about 129 deg.

Even though the logic circuitry was satisfied, there was no real error signal, and the roll axis was essentially in a drift mode with the jets firing at random, due to background noise. It turned out that the cumulative action was to cause the spacecraft to drift primarily in a direction of increasing clock angle. At some unknown time during the drift, the star Alderamin was acquired at a clock angle of 171 deg after drifting about 42 deg. Alderamin is about 0.05 times as bright as Canopus, with a bright background, and the error signals were too noisy to determine the time of acquisition.

At 334:13:12:34 GMT the spacecraft went into an automatic roll search. This loss of roll acquisition was the first of a series of losses of acquisition that eventually were realized to be caused by minute particles floating by and reflecting light into the tracker. This problem is discussed at length later. At 13:26:15 GMT after 13 min and 41 sec of roll search, the star Regulus was acquired at a clock angle of 278 deg. Lock was maintained on Regulus until the next day, since Canopus acquisition was not necessary to the mission at this time.

At 335:9:13:47 GMT, DC-21 (roll override) was initiated and the star Naos was acquired at 9:20:56 at a clock angle of 338 deg. Another DC-21 at 10:45:09 caused γ Velorum to be acquired at a clock angle of 343 deg at 10:46:00. Then finally Canopus was acquired by a DC-21 initiated at 10:57:57, and lock was obtained at 10:59:38.

c. Solar vane attitude control. Solar vanes were mounted on the spacecraft at the ends of each of the four solar panels to attempt to use solar photon pressure for pitch and yaw control.

The solar vane control system was designed to accomplish three things:

(1) Put the spacecraft center of pressure behind the center of gravity.

(2) Cancel unbalanced torques on the spacecraft in pitch and yaw.

(3) Damp out the limit cycle motion, in pitch and yaw, such that the angular motion will go to zero within the deadband of the optical system.

Considering (1), it is noted that, since the solar panels are on the side of the bus toward the Sun, there exists a situation which causes the solar force to try to flip the spacecraft around if the roll axis doesn't point precisely at the Sun. The solar vanes are mounted on the ends of the solar panels at a nominal angle of 35 deg from the plane of the solar panels, away from the Sun. This puts the center of pressure behind the center of gravity, and if the roll axis does not point at the Sun, there is a restoring torque to bring it back.

In consideration of (2), stepping motor actuators were employed to move the vanes about their nominal deployment angle to cancel out unbalanced torques on the spacecraft. The vane actuators will step 0.01 deg each time the switching amplifier pulses a jet. If a clockwise jet fires, the vanes move counterclockwise to reduce the torque that caused the clockwise jet to fire. In this manner the difference in the clockwise and counterclockwise pulses causes the vanes to gradually counterbalance the unbalanced torques.

Considering (3), it may be noted that the vanes are attached to the stepping motor actuators by means of bimetallic fittings that are exposed to the Sun through a slotted grid acting as a Sun valve. As the angle with

the Sun varies, the bimetal fittings are exposed to varying amounts of sunlight and the differential heating causes the bimetal to rotate the vanes. The direction of the rotation is such as to reduce the restoring torque. If the restoring torque were not reduced, the spacecraft would oscillate at a constant amplitude, depending upon the initial conditions. By reducing the restoring torque as a function of the angle, the amplitude of the oscillation is progressively decreased until it is damped out completely within the deadband of the gas-actuated system.

Solar vane acquisition. The first solar vane measurements were coincident with the turn-on of the adaptive mode actuators at the time of CC&S L-3 (initial star acquisition). At this time it was noted that the vanes had been deployed beyond the nominal position angle of 35 deg below the plane of the solar panels. They were deployed in the following positions:

$(+x)$ vane at 21 deg

$(-x)$ vane at 15 deg

$(+y)$ vane at 17 deg

$(-y)$ vane at 11 deg

The deployment failure was due to an unsuspected source of friction that was present during ground testing, but not present in the space environment. In spite of the overtravel, the center of pressure of the spacecraft is behind the center of gravity so that there is a net restoring torque of about 1.1 dyne-cm/deg about the pitch axis and 1.7 dyne-cm/deg about yaw.

The $(+x)$ and $(-x)$ vanes, which control the yaw axis, have been working properly in the adaptive mode by cancelling out an initial unbalanced torque of about 25 dyne-cm, probably due to the skewed angle of the high-gain antenna. The $(+y)$ and $(-y)$ vanes have not been observed in an operating condition. They are definitely in a failed mode. The most likely explanation is that the actuators are locked up electrically. The design is such that within the first 30 msec of actuator turn-on, if a jet fires, the actuator will lock. The telemetry data indicate that it is very likely that a jet did fire at that time.

Since the $(+x)$ and $(-x)$ vanes were operating in the adaptive mode to reduce the unbalanced torques, they were expected to operate eventually in the thermal mode to damp out the limit cycle. But it immediately became apparent that after the unbalanced torque was reduced to about 5 dyne-cm, the disturbance torques proved to be quite variable. In fact the torques will many times change by 1 or 2 dyne-cm between valve firings. Over longer periods, such as several days, the disturbance torques would vary as much as 5 to 15 dyne-cm. Now the maximum restoring torque of the spacecraft over the $\pm$½-deg limit cycle is 0.85 dyne-cm and the vane damping is 0.30 dyne-cm. (This is degraded performance due to overtravel at deployment). It is not possible for the thermal actuators to perform their function under these circumstances.

These varying disturbance torques are obviously not solar torques. At this time, it is felt that the best explanation is that they are due to the normal leakage of the gas valves. The normal valve leakage of 3.0 cc/hr at standard conditions will actually provide 16 dyne-cm per valve of torque, if it is assumed that the nominal gas laws apply. There are four valves controlling each axis, and the leakage has been observed in testing to vary with valve actuation. Therefore, even though the average leakage is known, it is obvious that the leakage, and hence the torques, could vary considerably over a period of time. If the seating characteristics of the valves change over a period of time, one would expect long-term variations in the disturbance torques, and as has been observed, if the seating for each valve firing is slightly different, then one would see short-term variations. It should be noted that this is a preliminary attempt at an explanation, and continuing data reduction may throw more light on the matter.

Since the long-term disturbance torques have varied, it is interesting to note that the $(+x)$, $(-x)$ vanes have been observed moving and cancelling out these disturbances in the adaptive mode of operation.

d. Midcourse maneuver. For the midcourse maneuver, the spacecraft attitude control is switched to an inertial mode by switching out the optical sensors and switching integrating capacitors around the gyros so that the control system is in a rate-plus-position mode, using the gyros for position information as well as rate. The commanded turns are accomplished by applying a timed, constant, calibrated current to the gyro torquers so that the spacecraft will turn at a fixed rate for the given time period. Two turns are necessary to arbitrarily point the midcourse motor thrust vector and *Mariner IV* used a pitch and then roll turn sequence.

First midcourse maneuver sequence. The start of the midcourse sequence (initiation of DC-27) took place at 339:14:35:00 GMT. This command turns on the gyros

for warm-up 1 hr prior to the start of the commanded turns. At 14:35:47 the gyros came on and started to spin up. The spin-up of the gyros causes a disturbance in the attitude-control system and the pitch, yaw, and roll error signals were driven over to one side of the deadband. The roll channel, which is of particular interest, started limit cycling against the negative side of the deadband with an angular excursion of 1 DN, which is a resolution of 0.41 mrad. After 49.3 sec of operation (eleven frames of data), a large transient was observed in the roll error channel equivalent to −16.0 mrad. The next data frame (4.2 sec later) showed the spacecraft going into automatic roll search, which continued until Earth-light reflections caused an acquisition to occur at 14:52:32 at a clock angle of about 90 deg.

The fact that the roll-error signal was forced to one side of the deadband by the gyro spin-up was a completely expected, normal event. The huge transient in the roll channel, and subsequent loss of acquisition, was catastrophic to the initiation of the maneuver and caused it to be aborted and postponed for one day. The one sample of roll error of −16.0 mrad is impossible to explain by actual spacecraft motion, because the impulse required is catastrophic and would have been observed in the pitch and yaw channels and on the roll gyro, which it was not. It appears that the signal was an electrical transient of some kind.

In view of the experience and analysis in connection with the loss of star acquisition in general (which generated the minute-particle theory as the cause of losses of acquisition), it seems that the loss of Canopus at the initiation of midcourse falls into the same category. It is postulated that the time correlation of gyro warm-up to subsequent loss of acquisition is due to the fact that the particles which were shaken loose from the solar panels by the gyro starting transient were then driven in front of the star tracker by solar pressure or spacecraft static charge. An instantaneous bright flash would cause a high brightness gate violation and a false error signal. Since the resolution of events in this mode is 4.2 sec, it is possible to miss getting a sample of the flash in the brightness channel.

The performance of the spacecraft at initiation of gyro warm-up prior to the start of the second and successful midcourse sequence was identical to the first except for the loss of acquisition.

Second midcourse maneuver sequence. The start of the second midcourse maneuver sequence (the successful one) took place at the initiation of DC-27 at 340:14:25:13 GMT. The gyros came on and the gyro spin-up caused the roll limit cycle to stay on the negative side of the deadband, as in the first maneuver try. It should be pointed out that this is normal. After the gyros were up to speed, the roll limit cycle was normal.

The maneuver consisted of a pitch turn of −39°.16 and a roll turn of +156°.07. The pitch turn starting transient was seen at 15:25:12 and the stopping transient at 15:28:54. The start roll transient was at 15:47:10 and stopping transient at 16:01:19. The turns were correct in every respect. The amount of overshoot in the rate plus position measurement seen during the starting and stopping transients was seen to be within the tolerances expected for the given control system acceleration of 0.45 mrad/sec. This is the only good confirmation available of the steady-state operation of the gas jets.

Autopilot performance. The pitch turn was −39°.16 deg and the roll turn was +156°.07 deg. These turn angles include a vernier adjustment in pitch and roll to compensate for a known center-of-gravity misalignment error. The action of the autopilot under the known center-of-gravity misalignment rotates the thrust vector to the proper direction in inertial space.

A vernier adjustment was also made to the motor-burn time to compensate for jet-vane drag. The compensation was based on the predicted initial conditions to the autopilot from the attitude-control system. On the basis of the commanded turn angles, it was expected that solar torques would keep both pitch and yaw angular positions held against the negative side of the attitude-control deadband. This initial angular offset causes the autopilot to drive the jet vanes hard over, which produces 6 lbf drag. The integral of the drag force over the transient period following motor ignition provides the magnitude of the motor-burn time correction. The actual position of the spacecraft in the pitch and yaw attitude-control deadband was exactly as predicted.

The midcourse rocket was ignited at 16:09:09.6 and burned for 20.4 sec. Four data points on the gyro signals were received during the motor-burn period. Although this did not provide enough data for a thorough analysis, three events of significance appear to fit the observed points. These are: (1) The first data point after motor ignition indicates a transient overshoot in pitch and yaw. (This would be expected from the known, initial conditions on the autopilot). (2) For the remaining three points during the burn period, pitch and yaw maintained an equal and opposite offset, indicating a center-of-gravity

misalignment angle of approximately 2.2 mrad or 0.064 in. (3) A very slow motion in the roll channel may have been a low-amplitude limit cycle due to friction in the jet vane actuators. This limit cycle is theoretically predictable and has been observed in analog computer simulations, but has not been observed in previous spacecraft, because of insufficient data during the midcourse maneuvers.

The entire midcourse maneuver and the performance of all subsystems were very satisfactory. Tracking data have verified that the *Mariner IV* midcourse was very accurate.

Reacquisition after midcourse. After the midcourse sequence is completed, the CC&S returns the attitude control to the normal Sun-star mode of control and automatic Sun acquisition takes place, with the Sun gate providing the logic for star acquisition.

Sun reacquisition was commanded by the CC&S at 16:15:10. Since the pitch turn was of such a small magnitude, the Sun acquisition was short, taking place at 16:21:07. Again the Sun gate field-of-view was seen to be 2°.2.

The Sun gate event started roll search for Canopus and the first star acquired was γ Velorum at 16:44:36 at a cone angle of 342°.8. Roll override was initiated at 16:52:50 and Canopus was acquired at 16:55:00 and regular roll control was established.

e. Cruise performance

Roll-control transients. The most noteworthy observation made during the attitude-control cruise portion of the flight was the fact that transients in the roll-control system caused the spacecraft to go into the automatic roll-search sequence. In some cases, a brightness transient was associated with the roll-error transient. Five of the roll transients were noted in the first ten days of flight.

After lengthy analysis and simulation, it was determined that the most likely and probable cause was that minute, bright particles were floating by the Canopus tracker and causing brightness transients which exceeded the upper brightness gate limits of the tracker. If the error signal in the tracker was negative, reacquisition would immediately take place, otherwise the automatic roll search took place. A flat specular particle of 0.005 in. diameter would give a brightness indication to the upper gate level (8 times Canopus) at a distance of 2500 ft from the sensor. The bright flashes are of short duration and the telemetry resolution is not good enough to sample them very frequently.

An investigation was performed to locate a possible mechanism for the generation of particles. It was discovered that extremely small meteoroids (approximately 10^{-3} g) impacting the spacecraft could cause the release of dust and lint in frequency of occurrence in the range to explain the observations.

It was recommended that DC-15 be used because it would remove the high gate from the control system logic circuitry. This was done at 352:17:30:00 GMT. Up to this date (April 9, 1965) the use of DC-15 has been very successful. Many roll transients have been observed, but none has caused a loss of acquisition. There seems to be little danger that a particle will cause the tracker to deflect from Canopus because the bright flashes from the tracker are of such short duration.

Minimum rate increments. In the limit cycle operation of the control system, the limit cycle rates are determined by a minimum rate increment established by a minimum on time circuit. The design goal for the rate increment was 9.0 μrad/sec.* In the pitch and yaw systems, the minimum rate increment turned out to be 18.4 μrad/sec and 14.0 μrad/sec in roll. The reason for this is still being investigated. It should be noted however, that the effect on the cruise gas consumption is negligible due to the large reserve available.

Attitude-control gas consumption. The rate of gas consumption used during the cruise mode is 3.76×10^{-3} lb/day $\pm 10\%$. As of April 1, 1965, the total weight remaining was 4.68 lb, yielding a lifetime of 3.4 yr at that date. This is well over the requirement.

Canopus tracker cone angle updates. As the spacecraft moves about the Sun, the cone angle of Canopus changes as a function of time. The total change is about 22 deg while the cone angle field-of-view of the star tracker is a total of 10 deg. Therefore, a CC&S program causes the center of the cone angle field-of-view to be switched periodically to new positions to follow Canopus. Two of these cone-angle updates have been commanded by the CC&S at 058:17:02:00 GMT, changing the cone angle from 100°.2 to 95°.7 and at 092:14:24:00 GMT, changing from 95°.7 to 91°.1. There was no observable transient in the roll-control system at the time of the updates.

*μrad = microradian

E. Spacecraft Design

1. Spacecraft Subsystems

a. Absorptivity standard. One of the problems that was recognized with the *Ranger* and *Mariner II* spacecraft designs was the difficulty in interpreting the temperature data collected during flight. With the limited number of measurement channels, it was possible only to determine the condition of the spacecraft and to indicate the adequacy of the temperature-control system. For example, it was clear that the *Mariner II* flight temperatures were much higher than expected, based upon analysis and testing in a space simulator, yet from the data that were received it was not possible to actually isolate the cause of the problem. A number of effects, or combination of effects, could have caused the same observed condition.

In the *Mariner C* design two steps were taken toward solving this problem. First, a significant increase in the number of temperature measurement channels was made possible by further subcommutating the data encoder. The time interval between data samples was considerably increased, but this was not considered to be a severe compromise because the temperatures during the long cruise to Mars would change very slowly. The second step taken to improve the data reduction capability consisted of providing a means of separating the variables associated with the spacecraft temperatures. The temperatures depend basically upon three things: (1) The internal power dissipated by the electronics, (2) the amount of energy radiated to space, and (3) the amount of energy absorbed from solar radiation. There was already a significant number of measurements which would indicate the status of the various subsystems of the spacecraft and give an indication of how much electrical power was being consumed. The energy emitted from the spacecraft is primarily through the electronic bays, and this was regulated by thermostatically actuated louvers. One louver blade of the set on each of three bays was instrumented to telemeter the opening angle, with care not to degrade the performance of the individual blades. Based upon ground tests, it would be possible to estimate the heat radiated to space. From the louver position readings and the electrical power measurements, it was anticipated that problems associated with these two variables which affect the temperature control system could be identified.

The solar radiation absorbed is the largest thermal input to the spacecraft temperature control system, (particularly the appendage items to the bus) and, unfortunately, is the most difficult to determine. To give a positive measure of this input, it was necessary to design an instrument which was able to measure the energy absorbed by typical surfaces used on the spacecraft. The case of an insulated flat plate in sunlight was selected as being the most useful measurement within the scope of a number of constraints that were imposed. With a sample surface radiatively and conductively removed from the spacecraft, it was possible to isolate the effect of the solar radiation on the temperature control of surfaces.

Design constraints. It was necessary to recognize the relative importance of this instrument, later named the "absorptivity standard," in the design of the spacecraft. Although valuable for evaluating the performance of the temperature-control system, the absorptivity standard would probably not provide any in-flight information which would improve the chance of a mission success. A possible exception to this was the case where one spacecraft was launched and a temperature-control problem observed before the second spacecraft was launched. However, when considering the difficulty of adjusting anything on the spacecraft during the relatively short firing period, this possibility appeared to be unlikely. Considering that the absorptivity standard is not required for mission success, a number of other constraints logically followed. If the absorptivity standard began to compete with more important areas (such as the temperature control of the spacecraft, due to weight, schedule, or manpower requirements), its priority would be clearly secondary. This priority, in turn, demanded that any interface with the spacecraft would be minimal. Specifically, no special circuitry was to be required by the data encoder, no electrical power was to be used, the weight was to be limited to approximately 1 lb, and it was generally not to compromise the spacecraft design in any way. In addition, the instrument was required to meet the type-approval, flight-acceptance, and quality-assurance standards.

The encoder constraint dictated that its interface be identical to the other standard temperature measurements. A major problem turned out to be associated with the uncertainties in the standard flight temperature measurements. An initial investigation of the accuracy required of the temperature measurements precluded any significant absorptivity data. Subsequently, a method was conceived which permitted a limited number of flight temperature measurements to the precision required. This was accomplished by telemetering the

UNCLASSIFIED

[redacted]

NATIONAL AERONAUTICS AND SPACE ADMINISTRATION

Space Programs Summary No. 37-33, Volume II

for the period March 1, 1965 to April 30, 1965

The Planetary–Interplanetary Program

(Title Unclassified)

Classification changed to UNCLASSIFIED
JPL - Letter from NASA - Langley
on Nov. 4, 1970, signed by W. E. Hanson
Date: Jan. 4, 1971 | By: A. Castaneda

JET PROPULSION LABORATORY
LIBRARY
JUL 1 1965
CALIFORNIA INSTITUTE OF TECHNOLOGY

Copy No. 484

JET PROPULSION LABORATORY
CALIFORNIA INSTITUTE OF TECHNOLOGY
PASADENA, CALIFORNIA

May 31, 1965

LAB B01074

[redacted]

GROUP 4 ... declassified after ... years.
UNCLASSIFIED

136625

action of a thermostat rather than a direct measurement of temperature. Within the weight constraint of approximately 1 lb, it was possible to measure the absorptance of four samples. A black sample was included as a measurement of the intensity of the solar radiation and to provide information on the stability of Cat-a-lac black paint after prolonged exposure to the space environment. A sample of JPL's most stable white paint was included because of the rather large uncertainties associated with this type of surface. White surfaces are known to yellow after prolonged exposure to ultraviolet, but the magnitude of this degradation was not known. A sample painted with aluminum silicon paint was included for similar reasons. In addition, it would give an indirect indication of the temperature of the attitude-control jets located at the tips of the solar panels. The fourth sample was one of polished aluminum. This was included primarily because of its wide use on the spacecraft as a temperature-control surface and as a verification that the ground tests with ultraviolet, and proton and electron bombardment of these surfaces were indeed valid.

Basis of data interpretation. In reality, the absorptivity standard measures the temperature rather than the absorptance of the surface. The instrument was designed in such a way that an expression ($S\alpha_s/\epsilon$) could be determined from the temperature measurement. ϵ and α_s are the emittance and solar absorptance of a surface exposed to the Sun, respectively, and S is the intensity of the solar radiation.

Relatively reliable measurements of ϵ are possible, using existing laboratory techniques; but this is not the case with S and α_s. This is because they vary with wavelength λ. More specifically

$$S\alpha_s = \int_{-\infty}^{\infty} (S_\lambda \, \alpha_\lambda) \, d\lambda$$

From a purely thermal consideration, it is not required to know more than just the product $S\alpha_s$, since the heat input is of the only importance in the thermal balance. However, there are at least two considerations requiring a separation of S and α_s. First, if either the solar intensity or the surface absorptivity changes with flight time, the temperature will also change. It is required to know how they vary and their relative contribution to predict the resulting change in temperature.

The second need to separate S and α_s is a practical one associated with a verification of the thermal design of a spacecraft. As space probes have become more complex, more emphasis has been placed on solar simulation tests. In these tests, the spacecraft is placed in a vacuum and heat-sink environment similar to space and illuminated with an arc source to simulate the Sun. The ideal space simulator test would find surfaces exposed to the simulated sunlight absorbing the same amount of energy as they would in space. Since the α_λ is not a constant, but is a complex function of λ, the α for a given surface in a given simulation is dependent upon the spectral distribution of the simulation. If all of the surface illuminated had only one treatment, the simulator intensity could be varied to compensate for the effective α of the surface in that light. It is not practical, except in the simplest cases, to constrain spacecraft design to a single surface treatment. The actual spacecraft has many different surface treatments with widely varying α_λ. Therefore, it is impossible to get proper heat inputs into all surfaces if the simulator spectrum varies from the solar spectrum. It is therefore important to determine the effective α of commonly used surfaces in the simulator as compared to the α of the surfaces in the actual sunlight. An examination of the errors associated with spectral measurements of both actual sunlight and solar simulation indicates the need for a direct experimental comparison of absorptance.

$S\alpha_s$ can be separated into S and α_s by either measuring S directly by a radiometer technique or by including a sample with a known α_s. The *Mariner* constraints precluded the first choice, and lack of a reference surface prevented the second choice. These two methods are approximated by the data from the black sample, and present knowledge of the solar intensity. The α_s for the black sample, determined in the laboratory, is felt to be trusted to $\pm 2\%$ and should not change much in space. The solar constant (solar radiation intensity at the mean Sun–Earth distance) is estimated to be known to $\pm$ 5%. Because of the instrument error in determining $S\alpha_s$, it should be comparably accurate to compute the α_s for the white, aluminum silicon, and polished aluminum samples by either assuming S is known, or by computing S based upon the black sample. Comparison of the results provides a check on the instrument performance and solar intensity. The absorptivity standard data will not produce any direct information about the spectral distribution of either the sunlight or the absorptance of the materials selected. Only an integrated value of $S\alpha_s$ will result. However, information will be implied indirectly about the spectral distribution of the solar radiation and α_s by how well the integrated flight and laboratory measurements of these variables agree.

Detail design description. Ideally, each sample surface should be a flat plate which absorbs solar radiation and

emits radiant energy from the front face only, i.e., perfectly insulated on the edges and the back. The absorptivity standard was designed to isolate the sample surfaces from radiation and conduction influences of the spacecraft. The sample surface in Fig. 1 is located on the end of a polished aluminum cylinder ①, which encloses the temperature transducer ⑥. The sample cylinder was mounted in a double conical support ②. Resistance to conduction was achieved by providing lightening holes in the cones and fabricating this support of plastic. Lexan, a polycarbonate plastic, was chosen for its high strength and low conductivity. All Lexan parts were coated with vapor-deposited aluminum to achieve a low emissivity.

The support cones were sandwiched between the Lexan cover ⑤ and the aluminum mounting ring ③. The cover served to block radiation from sources other than the Sun from reaching the sample. In addition, the lip overhanging the sample surfaces prevented stray and reflected sunlight from reaching the cavity between the sample cylinder and the support. The four sample assemblies were mounted in a row on a Lexan base ④ which in turn was located on the spacecraft upper ring structure above Bay 1.

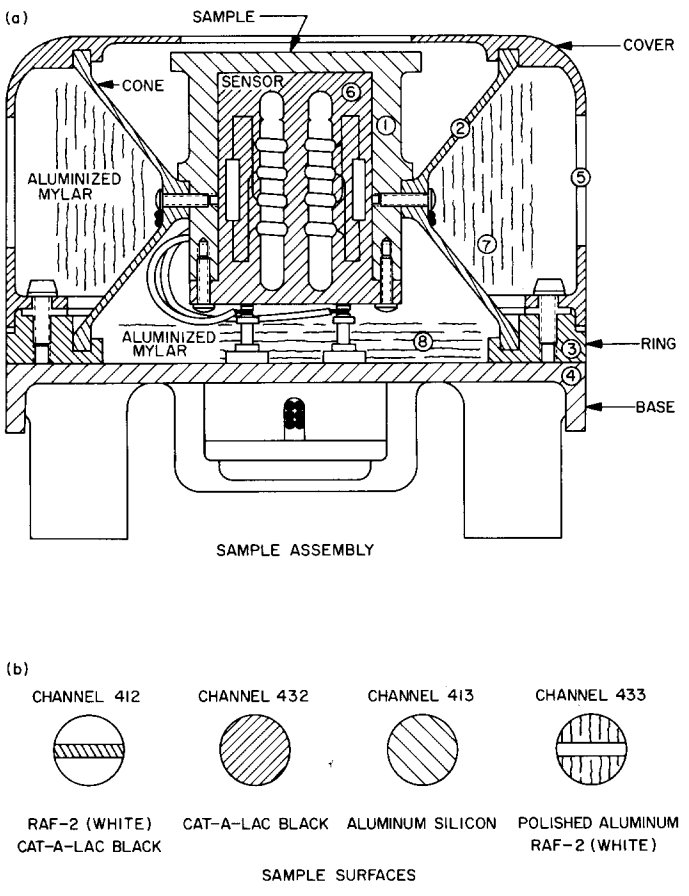

Fig. 1. Cross-section of absorptivity standard (a) sample assembly and (b) samples on absorptivity standard

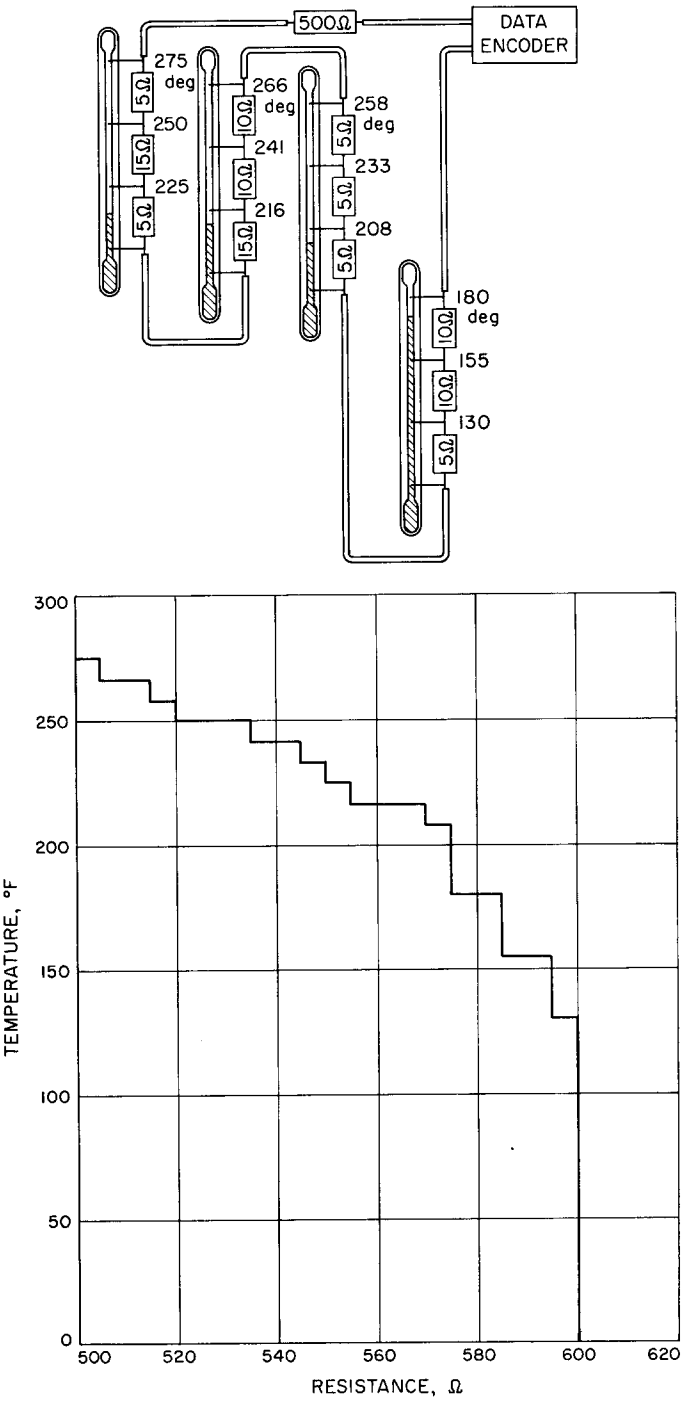

Fig. 2. Typical sensor signal versus temperature and sensor circuit

The sunlit areas of the covers and base were painted to give temperatures close to the sample temperatures to reduce gradients, and therefore heat exchange, with the sample. To reduce radiation interchange within the sample assemblies, the support cone was wrapped with aluminized Mylar ⑦ and disks of aluminized Mylar ⑧ were laid on the base. The wires from each sensor were wrapped around the support structure to prevent any heat losses through the wires from originating within the sensor itself.

The temperature sensors were each composed of 4 mercury thermometers and 13 precision resistors encapsulated in a glass-filled potting compound. Each thermometer, manufactured by the Philadelphia Scientific Glass Co., had four platinum wires passing through the glass wall to the capillary passage. Each thermometer was pressurized to 200 psi with hydrogen to reduce vibration sensitivity. The outer ends of the platinum wires were connected to rings, to which the circuitry was soldered. A typical sensor circuit is shown in Fig. 2. Combinations of 5-, 10-, and 15-Ω resistors bridge adjacent rings of each thermometer and the thermometers were wired in series with a 500-Ω resistor. As the sensor cooled the mercury in each thermometer receded, progressively making contact with fewer platinum wires (or advanced as the sensor heated, making contact with more wires). When the mercury thread bridges two wires, it shorts out the connecting resistor. Because the temperature at which the mercury touches or withdraws from a wire was known to 0.1°F, the step change in resistance of the sensor signaled a specific temperature. With three such steps per thermometer, a total of 12 temperature points per sensor was provided (Fig. 2). The total resistance range of each sensor was 500 to 600 Ω, which was compatible with the data encoder constraint.

The four samples, as mounted on the absorptivity standard, are shown in Fig. 1. A black stripe was added to the white sample to raise the temperature sufficiently to prevent freezing of the mercury in the thermometers as the spacecraft recedes from the Sun. A white stripe was added to the polished aluminum to decrease the sample temperature at the Earth solar intensity to a level compatible with the Lexan plastic. The temperature histories for ideal flat plate samples are shown in Fig. 3.

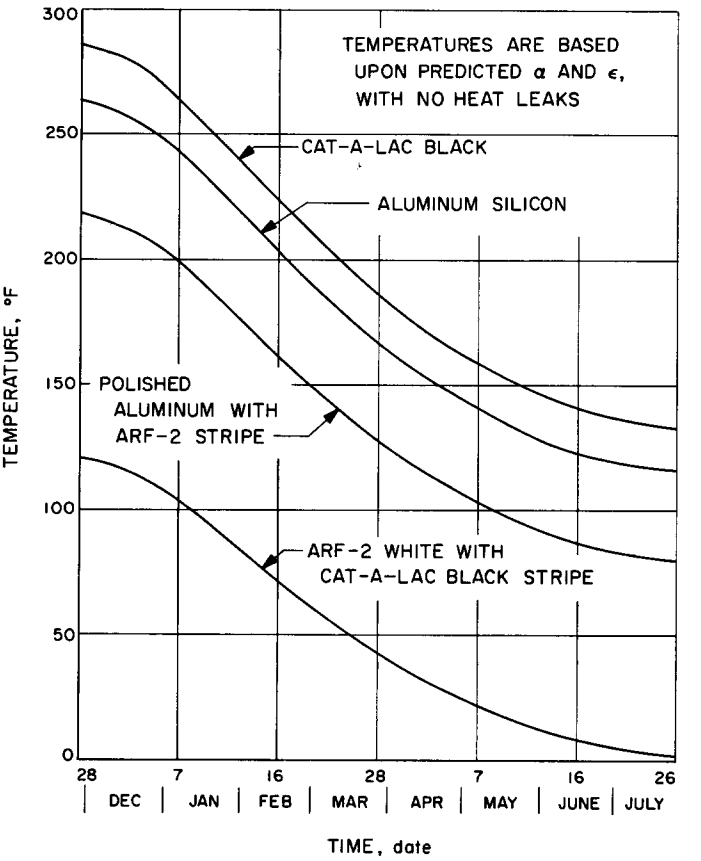

Fig. 3. Temperature history of ideal flat plate samples

Early flight results. The data received until the midcourse maneuver demonstrated that the absorptivity standard on *Mariner IV* was performing properly. All data numbers seen following launch and during midcourse were of nominal values and in the proper order. Two data points were seen during the steady-state cruise between launch and midcourse. The white sample warmed up one data step, although the solar intensity was decreasing. This is indicative of an increase in the solar absorptance of the white paint. This was substantiated when the polished aluminum sample also warmed one data step. The degradation of its white stripe more than offset the decrease in solar radiation intensity. A more complete analysis of this data and data following midcourse will be contained in a JPL Technical Report, "The *Mariner IV* Absorptivity Standard," TR 32-734 (to be published).

II. Voyager Project

A. Introduction

Activities of the *Voyager* Project during March and April have been devoted primarily to completion of the evaluations and preparations antecedent to award of the Phase IA Spacecraft Contracts. Concurrently, JPL technical support sections have initiated much of the technical study necessary to implement Phase IB and II Project activities.

The *Voyager* Spacecraft Source Evaluation Board presentation to NASA Headquarters was made on April 22, 1965, with subsequent selection of contractors by the NASA Administrator. Phase IA Contracts were issued to the following organizations on April 30:

(1) The Boeing Company, Aero-Space Division
(Major Subcontractors: Philco WDL, Electro-Optical Systems)

(2) General Electric Company, Missile and Space Vehicle Department
(Major Subcontractors: Motorola, Texas Instruments)

(3) TRW/Space Technology Laboratories
(Major Subcontractor: Douglas Aircraft)

These contractors are undertaking, in competition with one another, a preliminary design of a spacecraft system for the 1971 mission and a 1969 test flight. It is expected that the results of this activity will be available by the end of August this year. This study effort will be followed by a proposal cycle during which it is expected that two of the contractor participants will be eliminated from further project participation. It is planned that the remaining contractor will undertake the Phase IB and the Phase II effort.

At JPL, in addition to the project management activities which are now well under way, considerable attention has been directed to the completion of mission engineering studies in which to develop a model *Voyager* program that can best achieve objectives of the NASA program through 1977. These studies necessarily include investigations not only of spacecraft system considerations but also of capsule requirements. The scope of these studies includes both orbiter and lander missions.

Current propulsion studies are concerned with satisfying the functional requirements and configuration constraints of the two systems under consideration: (1) a liquid bipropellant system based on Earth-storable propellants for both midcourse corrections and orbit insertion and (2) a solid propulsion system for orbit insertion,

with midcourse corrections executed by use of a modified hydrazine monopropellant unit based on *Ranger* and *Mariner* experience. A propulsion development program involving participation from industry is currently under review.

In addition to study efforts in the areas of materials, telecommunications, guidance and control, system design, environmental requirements, instrumentation, test and launch operations, science, planetary quarantine, quality assurance, and reliability, the project is attempting to conclude arrangements for design and construction of the Sterilization Assembly Development Laboratory and the Experimental Assembly Sterilization Laboratory since both facilities will play a major role in ensuring that quarantine constraints affecting *Voyager* missions are satisfied. The System Test Complex for *Voyager* missions is also being studied in detail.

In addition, under the direction of the Project Office, all project elements located at JPL are reviewing existing Laboratory techniques and processes to evaluate their applicability to *Voyager* requirements.

B. Advanced Operational Support Equipment Development for Central Computer and Sequencer

The operational support equipment (OSE) development described here was started early in 1964 to support testing and operation of work on the advanced *Mariner C* type of central computer and sequencer (CC&S). Although work on the *Mariner* 1966 spacecraft has been stopped, development of the flight CC&S and its associated OSE was continued. The OSE test concepts and test techniques represent a significant advance from the equipment in use and will be applicable to future space missions, e.g., *Voyager*. The fabrication of the equipment is now nearly complete, and checkout and qualification tests are in progress. This report describes the test and design objectives, development, and operation of the support equipment.

1. Objectives

A brief review of the major objectives that resulted from analysis of support equipment requirements for the *Mariner* 1966, CC&S and other similar CC&S subsystems will give a better understanding of the test equipment.

a. CC&S testing capability

Versatility. The CC&S must be tested in the laboratory as a separate subsystem, tested on the spacecraft as part of the complete spacecraft system, and monitored at the launch complex during the launch count-down. It is desirable to have a single OSE which can be used in all test areas. This equipment must be sufficiently versatile to perform laboratory tests, special tests on the spacecraft, etc., in various sequences; or to perform new test sequences if the test results indicate such a need.

Previous test equipment automatically controlled the CC&S only on a fixed program of event times. If special tests, e.g., midcourse maneuver tests involving varying maneuver event times, were required, the tests could only be handled on a manual basis. If the fixed time for any CC&S event was changed, the OSE required a hardware modification to accommodate the spacecraft change.

A design objective for the advanced OSE has been to make any monitoring or control of a CC&S interface independent of time. Past OSE development schedules have been very difficult to meet, because of the uncertainty of the sequence of CC&S mission events and the associated times early in the design phase. This problem has now been totally eliminated by putting the OSE program on punched tape. If the mission events are changed, the OSE test sequence is modified by preparing a new tape. The time dependency results only after the test sequence has been programmed on the tape and read into the test equipment.

As in the past, the OSE configuration used to test the CC&S as a separate subsystem in the laboratory is the same as the system test set configuration used to test the CC&S as part of the spacecraft system in the spacecraft assembly area. The launch complex equipment is composed of certain assemblies that are also part of the system test set configuration. This launch support equipment now becomes much more versatile. The entire launch sequence can be made automatic, if this is desired. Thus, a single OSE design can be programmed to test the CC&S completely in any test area. Special tests are

accomplished by preparing new punched paper tapes to program the OSE. Multiple tests, such as performing several midcourse maneuvers one after another, are now possible.

Operational flexibility. Prior OSE designs have required external portable test equipment for OSE self-check; and it has not been possible to know the initial state of each CC&S interface when OSE main power was applied. The advanced OSE was designed to overcome these major operational restrictions.

The advanced OSE has an internal self-check feature with these advantages: (1) In both the laboratory and spacecraft test areas, all CC&S signals may be transferred to the OSE CC&S simulator. Any or all signal lines may then be qualified. (2) If a CC&S signal line fails to respond to OSE control during a laboratory or spacecraft test, a second mode of self check may be initiated that allows the transfer of all signal lines to the OSE CC&S simulator, except those required to stop and maintain the CC&S at a timing reference point.

The present OSE design automatically controls the initial state of each interface when power is applied, regardless of its last state prior to the power being turned off. When a change is commanded, the interface is monitored to see that the change takes place.

All prior CC&S OSE has printed out the mission sequence with the automatic cycling of the CC&S and required the operator to verify the printed tape visually to insure the correctness of the sequence. The possibility of human error and the time required to verify the printout manually are two disadvantages of this procedure. The advanced OSE eliminates these disadvantages by automatically verifying all CC&S signal changes. If the signal change is verified there is no printout, thus reducing the amount of printer tape that must be read and the wear on the printer mechanism. If, however, a particular test requires that a printed tape be generated for record purposes the OSE can be programmed to generate a printed tape containing all CC&S events and their time of occurrence. The operational features of the OSE are described in more detail later in the report.

b. Design simplification. One design objective has been to reduce the number of different components and circuits to as few types as possible to achieve greater reliability and maintainability.

Standard circuits. Past experience has pointed out the desirability of having only a small number of different logic circuits (gates, flip-flops, one-shot multivibrators, etc.) and special purpose circuits (relay drivers, light drivers, interface buffers, etc.). It has been a development objective to implement all logic networks around a single type of *nand* gate circuit. All functions have been obtained through the use of combinational or sequential network synthesis techniques. Excluding commercially supplied equipment, such as printers and tape readers, power supplies, and special purpose CC&S interface buffers, the only other circuit type used in the OSE is a standard indicator light driver.

By concentrating on standard circuits the circuit design was thus reduced to the logic circuit and the light driver mentioned above. These designs allowed the objective (to have as few component types as possible in the OSE design) to be achieved. Thus eight different circuit component types account for approximately 90% of the electrical components in the OSE. Reducing the number of component types has saved time and expense in procurement; and the small number of circuit types has simplified the design and qualification effort.

It is expected that by minimizing the circuit types, greater reliability and maintainability can be achieved in this OSE. Fewer types of spare circuit cards will be required in the inventory for repair.

Mechanical adaptability. Simplified construction, assembly, and ready access for servicing have been prime support equipment fabrication objectives for some time. The mechanical fabrication has been greatly simplified by using a great many circuit cards and circuit card files. This type of construction reduces each assembly to (1) chassis, (2) front panel, (3) printed circuit cards, and (4) printed circuit card files. Each of the subassemblies may be completely assembled, wired, and qualified independently of all other subassemblies.

This type of construction is flexible and allows for expansion or reasonable modification. Thus the equipment meets the objective of providing equipment which can be easily converted to a new task. The present equipment, fabricated without unreasonable expense and complexity, could be used in future spacecraft programs that might use a CC&S typical of those supplied in the past for *Ranger, Mariner II,* and *Mariner IV.* The advanced OSE is capable of testing any past or future CC&S which has up to twice the *Mariner* 1966 CC&S control capability

by making the following changes: (1) replace identification lenses in proper control switches, (2) add or remove any printed circuit subassemblies as required.

The needs of a future spacecraft program can be met by electrical redesign of two assemblies of thirteen in the test equipment: (1) the CC&S simulator assembly, which simulates the CC&S interface when the OSE is being qualified during a self-check; and (2) the transfer assembly which contains the necessary buffering circuits to mate to the CC&S.

The improved OSE was also fabricated to meet trouble-shooting and maintenance objectives:

(1) Signal flow diagrams of each logic network have been compiled to reduce the time required to localize any failure.

(2) All CC&S signal lines may be monitored from test points except control lines for manual command of CC&S relays. These test points are located in an assembly containing the CC&S buffering circuits.

(3) All assemblies are placed on slides and have quick release locks, except for some commercially supplied equipment that would be removed from the OSE for servicing.

(4) All assemblies which have a large number of front panel controls are constructed so that the front panel folds down on hinges for easy access to the rear of the panel.

(5) A new method of cable routing allows a greater degree of freedom in moving assemblies on slides in and out of the main rack.

2. OSE Description

The advanced OSE was fabricated in 13 assemblies mounted in two 6-ft racks. The placement of the assemblies is shown in Fig. 1. The assemblies in the left rack are, from top to bottom: (a) data processor logic, (b) CC&S simulator, (c) CC&S manual command, (d) data processor control, (e) drawer, and (f) signal transfer. The assemblies in the right rack are, from top to bottom (a) 2.4 kc power supply, (b) tape reader, (c) oscilloscope, (d) printer, (e) counter, (f) comparator, and (g) main power supply. The primary use and functional capability of the assemblies are more easily discussed if the assemblies are grouped as shown in Fig. 2.

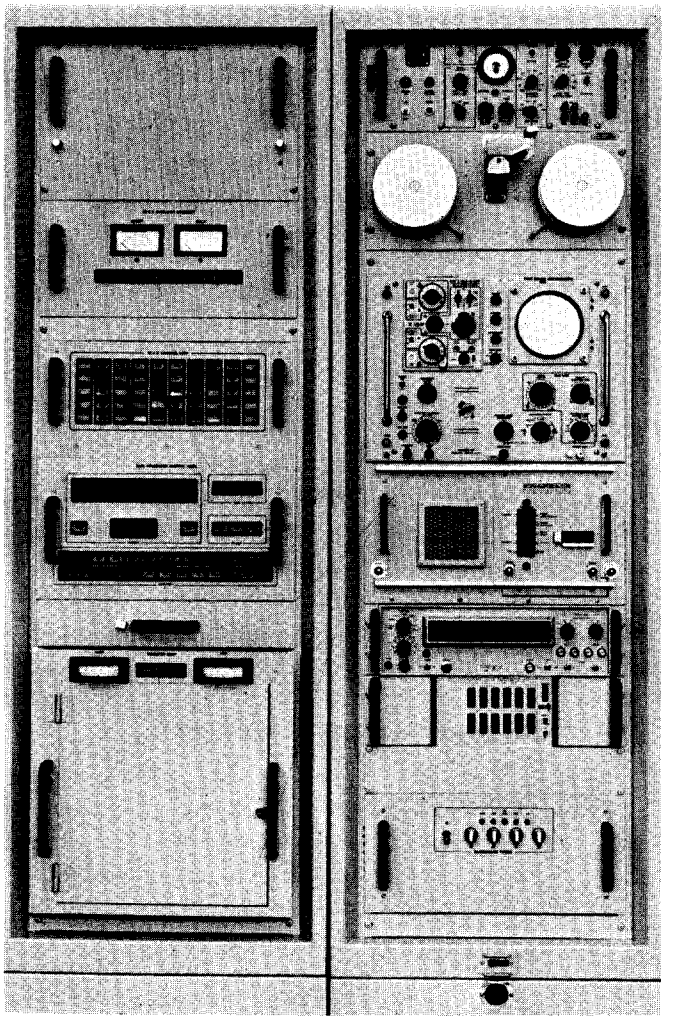

Fig. 1. Advanced *Mariner* OSE

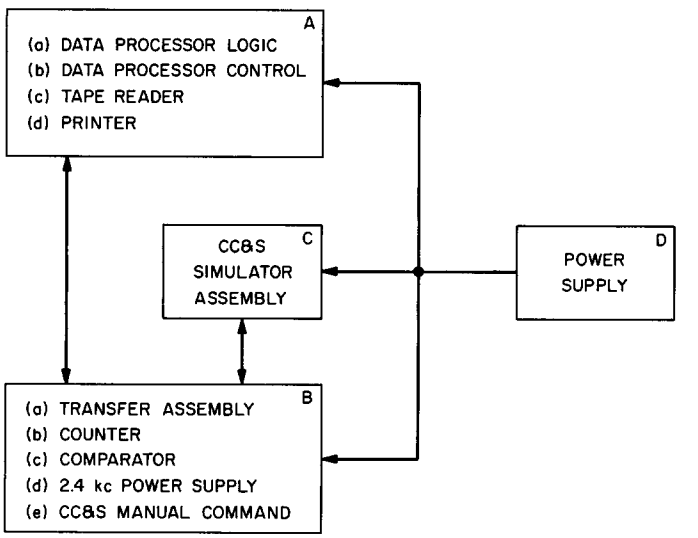

Fig. 2. OSE functional description

UNCLASSIFIED [redacted]

a. Block A assemblies. The purpose of these assemblies is to provide the OSE with programmable control. This follows from the general OSE requirements to provide a source of command control and data evaluation for the system under test. The CC&S OSE designs in the past have been of a special nature in that the command and data evaluation requirements have been tailored to a particular CC&S design. In the advanced OSE, however, the assemblies in Block A provide a programmable test capability that could be used for any past CC&S as well as any electromechanical system which has control and evaluation requirements within the capabilities of the present assemblies.

The major capabilities of these assemblies are as follows:

(1) There are 44 programmable command sources. If desired, this capability could be increased to 3,000 by adding standard logic networks.

(2) There are 88 programmable data points available for evaluation. This capability could be increased to 300 by adding standard logic networks.

(3) A six-place decimal counter is available to evaluate analog or digital information. Hence, with proper conversion, analog or digital data may be evaluated visually or by programmable tolerance measurements. The counter accepts input information at rates up to 500 kc.

(4) The tape reader uses a 16 channel tape. Five channels are used for address and 11 for information. As many as 10 commands can be given at a programmed event. The reader operates at rates up to 60 words/sec.

(5) It is possible to run tests in synchronism with external inputs. Any desired test program may be executed in part or entirely in synchronism with the external input.

(6) The printer documents test data for evaluation. The printer is presently capable of printing 8 channels of coded information at a rate of 20 lines/sec.

b. Block B assemblies. These assemblies provide the necessary buffering between the universal processing equipment (Block A) and the CC&S or the CC&S simulator. All special purpose interface circuits, logic, and the timing requirements are accomplished with these assemblies. Provisions have been made for about 250 lines from the CC&S direct access connectors, the launch cabling, and spacecraft users. Spares (10 to 15%) are provided in the cabling between assemblies.

c. CC&S simulator. The CC&S simulator provides an interface to the test equipment that is exactly like, or closely simulates, the CC&S. This assembly is capable of simulating a CC&S of approximately three times the interface presently used.

3. OSE Operation

a. Preparations. Prior to testing a CC&S, certain preparations must be completed for each mode of operation. The OSE has both manual and automatic testing modes. For the manual mode of operations step-by-step test procedures must be available. For the automatic mode a punched paper tape is needed. The step-by-step procedures for the manual mode are similar to those used on past spacecraft programs to check the CC&S sequence. These are described in *SPS 37-21* and *23*, Vol. II, and are not discussed further here.

The efforts required to produce an automatic taped program include:

(1) Development of a detailed program that describes each CC&S input command and each CC&S output signal as they will occur during the automatic test.

(2) Coding this detailed program into a series of words that defines the operation of the OSE.

(3) Preparation of a punched paper tape from the coded program by an operator using a tape preparation system.

(4) Verification and duplication of the tape.

(5) Storage for future use.

b. CC&S testing. The use of the OSE for CC&S testing is described with the aid of the functional block diagram shown in Fig. 3. When an operator tests a CC&S, he first determines the mode of operation to be used. If the operation is manual, he obtains the applicable manual test procedure and uses the equipment shown by the manual program control block in Fig. 3 to perform the test step-by-step. If the operator wishes to perform an automatic test, he selects the test tape and a general test procedure which describes how to perform automatic tests. The operator installs the test tape on the tape reader and starts and stops the tests with controls in the automatic program control block. The switches S1 through S6 would be in the positions shown in the block diagram for an automatic test. (The positions of S1 through S6 must be reversed for a manual test.)

UNCLASSIFIED

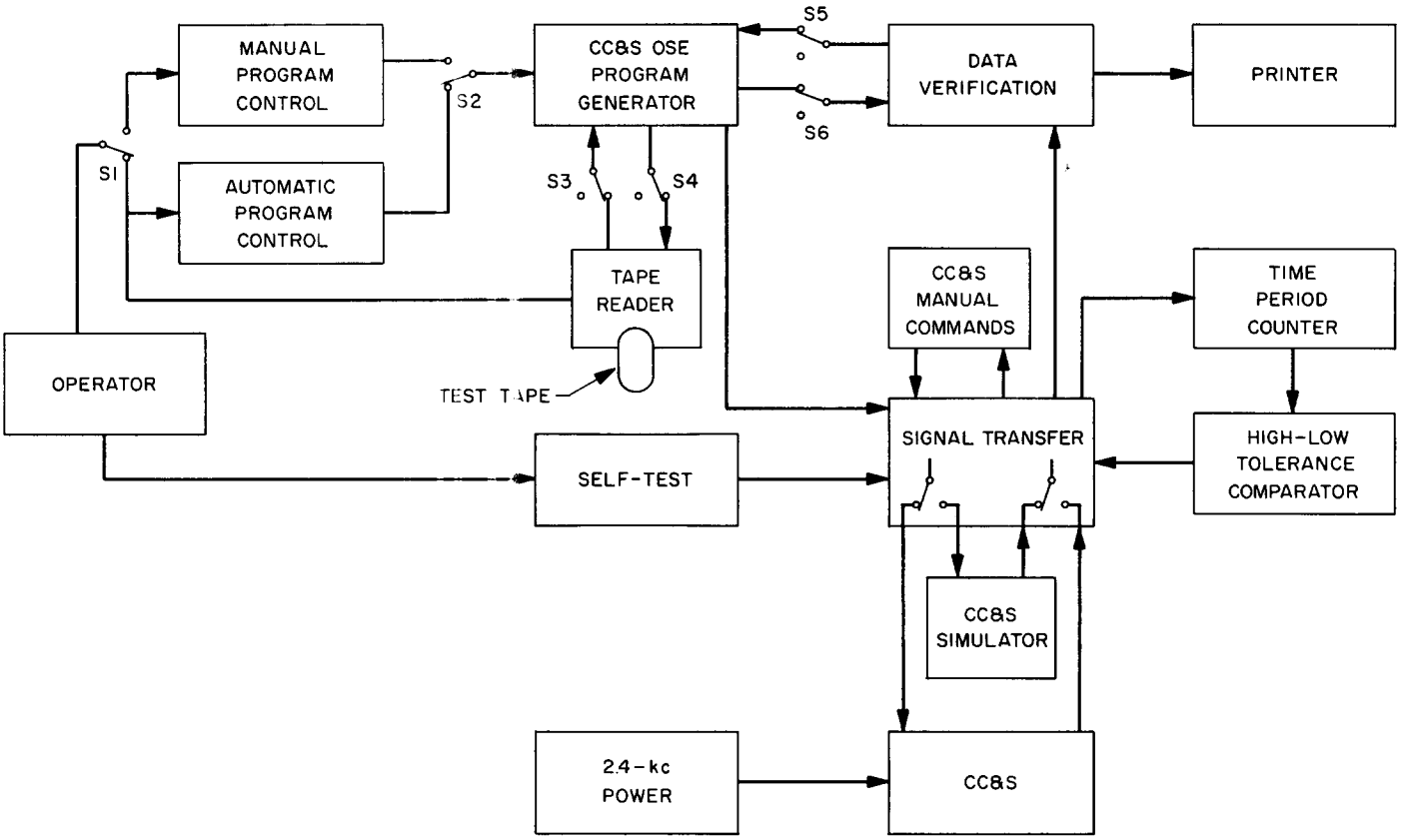

Fig 3. OSE functional block diagram

The automatic operation of the OSE includes the following steps (refer also to Fig. 3):

(1) Test information is taken from the test tape by the tape reader and sent to the program generator.

(2) The program generator decodes the tape information and sends control signals to the signal transfer assembly. The control signals are conditioned in this assembly and directed to the CC&S. The signal transfer assembly continually monitors all CC&S output signals. When a CC&S output changes as a result of an input control signal the signal transfer assembly receives this information, conditions it and passes it on for verification.

(3) The CC&S output change, after being conditioned in the signal transfer assembly, is directed to the data verification circuits. During the interval between the time the CC&S receives a control signal and the time it generates the output change, the predicted CC&S output change information is taken from the tape by the tape reader, sent to the program generator and there directed to the data verification circuits. If the actual CC&S response agrees with the predicted input, the program generator is notified of the agreement. The program generator then directs the test to proceed.

(4) If an error occurs during or before a data verification, the program will stop and the error will be printed by the printer. The printer may or may not print a CC&S output change during proper operation, depending on the control setting of the automatic program control.

Errors, however, detected in any of the various testing modes are printed out in a similar fashion. A time interval measurement is one example of this operation. The time period counter and high-low tolerance comparator are used to test or measure a periodic waveform for accuracy. The periodic waveform is directed to the time period counter. An out-of-tolerance condition may be detected by the high-low tolerance comparator which monitors all counter decades. If an out-of-tolerance measurement occurs at the end of a counting interval for the input waveform, the failure indication is directed to the signal transfer assembly. The failure is next recognized by the data verification circuits which cause the printer to record the time of failure.

UNCLASSIFIED

(5) To perform the OSE self test, the operator selects the self-test mode. The self-test control equipment commands the signal transfer assembly to transfer the appropriate signals to the CC&S simulator. There are two modes of self test (as mentioned earlier), and the lines transferred to the simulator are selected according to the mode in use. The response from the CC&S simulator is treated much the same as the CC&S response, and any error in operation stops the tests and prints the error.

(6) The individual CC&S relays may be controlled, using the equipment of the CC&S manual command block. An appropriate signal is generated in the CC&S manual command and directed to the signal transfer assembly and on to the CC&S. The response of the relay is directed to the signal transfer assembly, where it is conditioned, and then sent to the CC&S manual command, where the operator is provided with a visual indication of the relay state.

Table 1. Assembly location of OSE functions

Assembly	Block
Data processor logic	Automatic program control
	Data verification
	CC&S OSE program generator
CC&S simulator	CC&S simulator
CC&S commands	CC&S manual commands
Data processor control	Manual program control
Signal transfer	Signal transfer self test
2.4-kc Power	2.4-kc Power
Tape reader	Tape reader
Printer	Printer
Counter	Time period counter
Comparator	High-Low tolerance comparator

c. Assembly identification. The functional operations described by the block diagram do not correspond exactly to assemblies shown in Fig. 1. The location of these circuits or various functional blocks are related to the OSE assemblies in Table 1.

4. Development Status

Further material on the advanced CC&S support equipment will be presented in future issues of the *SPS* after final testing and delivery of the equipment. Equipment fabrication is now nearly complete, and checkout and qualification tests are in progress. The OSE has been mated with the CC&S breadboard and several interfaces are being modified to insure compatibility.

There have been very few wiring and fabrication errors, design errors, and other discrepancies. The equipment operation to date has been most satisfactory, and no difficulties are foreseen in completing checkout.

III. Future Projects

A. Asteroid Belt and Jupiter Flyby Mission Study

The final report of the subject study, conducted by Lockheed Missiles and Space Company under JPL Contract 950871, was received during February 1965. A summary of the objectives and results of the study is provided below.

1. Study Objectives

The prime objective of the study was to determine alternate ways of reliably accomplishing the following scientific objectives, separately, utilizing unmanned spacecraft.

(a) Measurement of the particle distribution encountered in traversing the Asteroid Belt within a corridor comparable in diameter with that of the spacecraft, and over a region 100 times the spacecraft diameter.

(b) Measurement of the physical and chemical surface properties of a statistically significant sample of asteroidal material.

(c) Observation of the gross surface features of one of the major asteroids within the belt.

An additional objective was to use the results of the Asteroid Belt study as growth potential to formulate a Jupiter flyby mission to obtain the following planetary environmental data: magnetic field, radiation, atmospheric pressure, temperature and composition, surface temperature, and visual.

The following tasks were to be performed in support of the objectives:

(a) Define functional requirements for accomplishing each of the mission objectives.

(b) Examine alternate system and subsystem concepts, perform tradeoff analyses, and suggest those concepts most suitable for fulfilling mission requirements.

(c) Perform failure mode and reliability analyses and apply the results to the selection of system concepts and the estimation of the probability of mission success and meeting partial objectives.

(d) Provide descriptions of each system concept together with functional specifications to ensure meeting mission requirements.

(e) Prepare development plans for all system concepts and provide preliminary cost estimates; cost and schedule data to include further study, design, development, manufacture, testing and flight operations.

(f) Define study concepts in sufficient detail to allow comparison with the *Mariner* Mars 1964 spacecraft.

2. Study Constraints

The following guidelines were used in the study:

(a) Mission period for particle distribution and composition mission to be 1967–1975. Major asteroid and Jupiter missions to be 1970–1980.

(b) Mission energy requirements to be compatible with *Atlas/Agena D* and *Atlas/Centaur* vehicles. A third stage to be used if required.

(c) Full Deep Space Instrumentation Facilities to be utilized.

3. Methods of Approach

Definition of the major functional requirements for successful accomplishment of the scientific objectives of each mission evolved from two basic and related areas: mission concepts and flight trajectories, and system concepts, associated subsystems, and application to spacecraft design.

a. Mission concepts. Flythrough missions to measure particle distributions, and physical and chemical properties of the particles have the simplest mission profiles. The trajectories lie essentially in the plane of the ecliptic and a launch can be made on any day. An infinite number of trajectories are possible but, for the purposes of the study, trajectories with aphelia at 3.2, 4.0 and 6.7 AU were examined. The first two provide long-term measurements of specific regions of the belt, and the 6.7 AU mission represents a relatively rapid survey of the whole region to beyond the orbit of Jupiter.

Two major asteroids, Ceres and Vesta, were chosen as suitable targets for observing gross surface features. The choice of two asteroids provides a greater degree of flexibility in planning the eventual missions, since the requirements are similar and the launch opportunities are interspersed. A miss distance at the target of about 1000 km is desirable for scientific observation.

A flyby of Jupiter represents a fairly conventional mission concept. The main variables are concerned with the encounter phase when various approach trajectories can be utilized to give the required coverage of the planet. Because of Jupiter's large mass, an approach to about 2 radii of the planet's center results in a dark-side passage for trips of moderate duration.

b. System concepts. A range of possible system concepts exists for each mission depending on the depth of scientific investigations attempted and the degree of sophistication adopted in the subsystem design. For the asteroid missions, the upper and lower ends of this range were examined. Minimum missions were defined for

Table 1. Alternate system concepts

Mission	Control mode	Typical science package[a]		Science payload, lb	Data transmission, bit/sec	Average total power requirement, w	Spacecraft weight, lb
		Distribution	Composition				
Asteroid Belt flythrough (Particle distribution)							
A1 Minimum	1 Spin stabilization only	Aa	Ba	18	1 (at 3.5 AU)	110	346
A2 Intermediate	2 Intermittent all-axis	Ab	Ba	28	9.8 (at 5 AU)	138	485
A3 Maximum	3 Continuous all-axis	Ad	Bb	65	30 (at 5 AU)	194	1,049
Major Asteroid Flyby							
C1 Minimum	1 No stabilization to target; All-axis stabilization for maneuvers, encounter, and data playback	Ca		6	17 (at 3.7 AU)	200	605
C2 Maximum	2 Continuous all-axis stabilization	Cc		75	56 (at 3.7 AU)	285	1,140

[a] Defined in Table 2.

which simple system concepts could be envisaged that would deliver small scientific packages with minimal demand on the subsystems. More refined system concepts, at least comparable in complexity to *Mariner C*, were also developed to give a capability of more comprehensive scientific observations to fulfill the requirements of maximum missions. System concepts for the performance of a Jupiter flyby were developed from those suitable for the maximum asteroid missions. Table 1 summarizes the alternate concepts studied. Table 2 gives the range of typical science packages for asteroid missions.

Table 2. Range of typical science packages for asteroid missions

Mission	Package No.	Instrumentation	Weight, lb	Power, w	Control mode	Evaluation
Particle Distribution						
A1	Aa	12 Impact gages for flux measurement (direction and number) spacecraft diameter	18	1.8	Spin[a]	Wide field-of-view, low angular resolution, reduced data rate
A2	Ab	6 Impact gages, flux ~ spacecraft diameter. Optical meteoroid detector, flux ~ 100 spacecraft diameter	19	5.9	Intermittent all-axis	All-axis stabilization for optical detector
	Ac	Multiple film meteroid monitor, flux ~ spacecraft diameter	30	5.0	Spin	Wide field-of-view, reduced sample rate
A3	Ad	Multiple film meteoroid monitor, optical meteoroid detector, impact gages, interplanetary instrumentation	65	17.6	Continuous all-axis	Continuous observation, maximum useful data, high reliability
Particle Composition						
	Ba	Impact mass/flash spectrometer	40	15	Spin	Wide field-of-view, low sample rate
B3	Bb	2 Impact mass/flash spectrometer (1 at standby), interplanetary instrumentation	105	22.6	Continuous all-axis	Continuous observation in direction of main stream, good reliability
Major Asteroid Flyby						
C1	Ca	Low resolution visual TV	6	15	All-axis for maneuvers, encounters and playback. Otherwise no stabilization required	Size and shape determination, some surface details, low data rate
	Cb	Low and high resolution visual TV	36	30	As above	Good detail, high data rate
C2	Cc	Low and high resolution visual TV, photometer/polarimeter, IR radiometer, interplanetary instrumentation	75	50.6	Continuous all-axis	Maximum useful data

[a] About axis perpendicular to plane of ecliptic.

4. Major Factors Affecting Mission

a. Scientific requirements. A comprehensive survey of desirable scientific observations, experimental techniques, and instrumentation showed that the most problematic mission would be the Asteroid Belt flythrough. Present instrumentation for the measurement of particle distributions such as microphone gages, pressure cans, etc., do not appear to be adequate in terms of the completeness of information provided and from the point of view of accuracy and operating life. No really suitable instruments exist for the measurement of the physical and chemical properties of asteroidal material. Thus a number of conceptual instruments are suggested. These are: multiple film meteoroid monitor, optical meteoroid detector, and impact mass/flash spectrometer.

Enough effort was devoted to prove the feasibility of these concepts but considerable development is required to perfect the technique, evaluate hidden problem areas, and calibrate the devices. All of these instruments are heavy, an obvious disadvantage, but would give good returns when evaluated in terms of information per pound.

The flyby mission to observe a major asteroid, on the other hand, could employ fairly conventional instrumentation, such as TV and radiometers and no development problems are envisaged. Extension to a Jupiter flyby is possible using some of the major asteroid-mission basic equipment, but the total instrumentation weight is increased because of the added observation requirements. The value of TV coverage of Jupiter's cloud-covered surface has been weighed. It can be argued that the TV pictures will be difficult to interpret and provide very little information return for the added complexity of data handling. On the other hand, visual observations would be invaluable for examining unexpected phenomena, such as gaps in the cloud layer or other observable features. For this reason two scientific packages were examined—with and without TV instrumentation.

It is far too early, of course, to make a definitive selection of scientific instruments. Typical scientific packages were selected for the various design studies. One important need for caution should be mentioned. The design of instruments to give statistically significant information on particle distributions and properties in the Asteroid Belt is very sensitive to the actual particle flux that will be encountered. This is an area of extreme uncertainty. Values of particle flux assumed for the instrumentation study were those suggested in the guidelines. They represent a likely upper estimate. Assumption of some lower value would lead to a reappraisal of the designs and scaling of the instrument geometry.

b. Trajectory data. Detailed trajectory analyses were performed for all missions. The results were used to establish energy requirements, mission profiles, and performance parameters. For the latter deductions, nominal spacecraft weights of 1000 and 1300 lb were assumed for the asteroid missions and Jupiter flyby, respectively. These values tend to be representative of system weights associated with maximum missions.

Characteristic velocities for the flythrough missions vary from 39,200 to 48,000 ft/sec for a range of aphelia from 2.0 to 6.7 AU. The major consideration is the duration of the mission, which can exceed 2 yr. The three basic parameters—trip times, aphelion distance, and velocity requirements—are interrelated. Rapid transits of the belts (outward leg) can only be achieved by high-energy missions that take the spacecraft to great distances from the Sun. Lower energy missions place the spacecraft in smaller elliptical orbits about the Sun, permitting a better (circumferential) survey of a particular region. However, the times are longer than necessary for adequate observations and might be excessive for system reliability. If the total mission is envisaged as consisting of outbound and inbound legs, which is advantageous in terms of the observation regions covered and backup information obtained, the above conclusions are reversed. Another important consideration, which can affect instrument design, is that the higher energy missions involve greater particle velocities relative to the spacecraft, except near aphelion where the relative velocities are essentially the same. However, the governing factor in the ultimate tradeoff will be launch vehicle availability. A summary of the relevant mission parameters is given in Table 3.

Launch opportunities for missions to Vesta and Ceres occur roughly every 16 and 15 months, respectively; thus, low-energy missions are possible on eight occasions for Vesta and nine occasions for Ceres in the period 1970–1980. Since velocity requirements for any of these missions do not vary greatly (Vesta, 40,000–43,000 ft/sec, Ceres, 42,000–44,000 ft/sec), trip duration is a valuable comparison parameter. A certain periodicity in desirable missions is then evident — every other opportunity showing a maximum or minimum trip duration for Ceres. Further, in general, the years for long flight times to Ceres coincide with short flight times to Vesta (Fig. 1).

Table 3. Asteroid Belt flythrough missions

Mission	ΔV^a, ft/sec	Time to aphelion, days	Time between radii, days				Relative velocity, ft/sec	Adequate launch systems for 1000-lb payload
			2.0-2.6	2.6-3.2	2.6-4.0	3.2-4.0		
Aphelion at 3.2 AU	17,200	570	220	560	—	—	17,000 3.2 AU	1, 2
Aphelion at 4.0 AU	18,800	720	160	240	960	730	30,000 3.2 AU 18,000 4.0 AU	1, 2
Jupiter Mission	22,300	1355 (600)[b]	120	150	390	240	45,000 3.2 AU 38,500 4.0 AU 29,000 5.2 AU 18,500 6.6 AU	1

[a] Injection from 100-nm orbit.
[b] Time to Jupiter's orbit.

This fact, together with the sequential launch opportunities, illustrates the flexibility available from considering more than one target asteroid. Minimum trip times (230 days for Vesta in 1978 and 420 days for Ceres in 1976) are still relatively long. Times associated with other years can be considerably longer. On this basis, apart from 1971 and 1976, Vesta missions look more attractive than those to Ceres. The 1976-Ceres and 1978-Vesta missions are also favorable (though not optimum) when other constraints such as velocity requirement, passage speed, etc., are considered (Tables 4 and 5). For earlier missions, the opportunities occurring in 1971 (Ceres) and 1972 (Vesta) appear attractive, although the velocity requirement for the Vesta trip is a maximum for the minimum energy possibilities.

As a means of reducing trip times, higher energy missions can be visualized. For a given payload weight, a launch system can be chosen that gives higher departure speeds. With a nominal payload of 1000 lb and a characteristic velocity of 49,150 ft/sec, Ceres and Vesta mission durations are considerably reduced — to around 200 days over the whole decade. Such an approach, if possible, gives more flexibility to planning a future program.

Jupiter flyby missions are governed by similar factors that affect the major asteroid mission, with some exceptions. There is less spread in trip times for minimum energy conditions but a greater variation in trip time through a 30-day launch window. Velocity requirements are much larger (46,000–49,000 ft/sec) and trip durations are about 2 yr. This value can again be reduced by employing a high-energy launch system.

c. System design. Detailed design studies were performed on conceptual spacecraft to satisfy maximum and minimum missions to the Asteroid Belts and a maximum flyby mission of Jupiter. A minimum flythrough mission (particle distribution) utilizing a spin-stabilized system concept results in a spacecraft weight of 346 lb. The minimum flyby of a major asteroid can be performed with a spacecraft weighing 605 lb. This system is intermittently stabilized (3-axis) for critical maneuvers such as midcourse corrections, encounter and playback; otherwise, no stabilization is required. The maximum mission concepts result in the following system weights: 1049 lb (particle distribution), 1097 lb (particle composition), 1140 lb (asteroid flyby) and 1289 lb (Jupiter flyby). Thus a range of possible payloads is represented that can be traded off against data-gathering requirements and the availability of suitable launch vehicles.

A summary of spacecraft weights is contained in Tables 1, 2, and 6 to 8. For the maximum missions, weight increases result mainly from control requirements (continuous all-axis stabilization over long flight periods), large data rates, and high power requirements. Structure weights are high, due partly to the need for protection

[redacted] UNCLASSIFIED

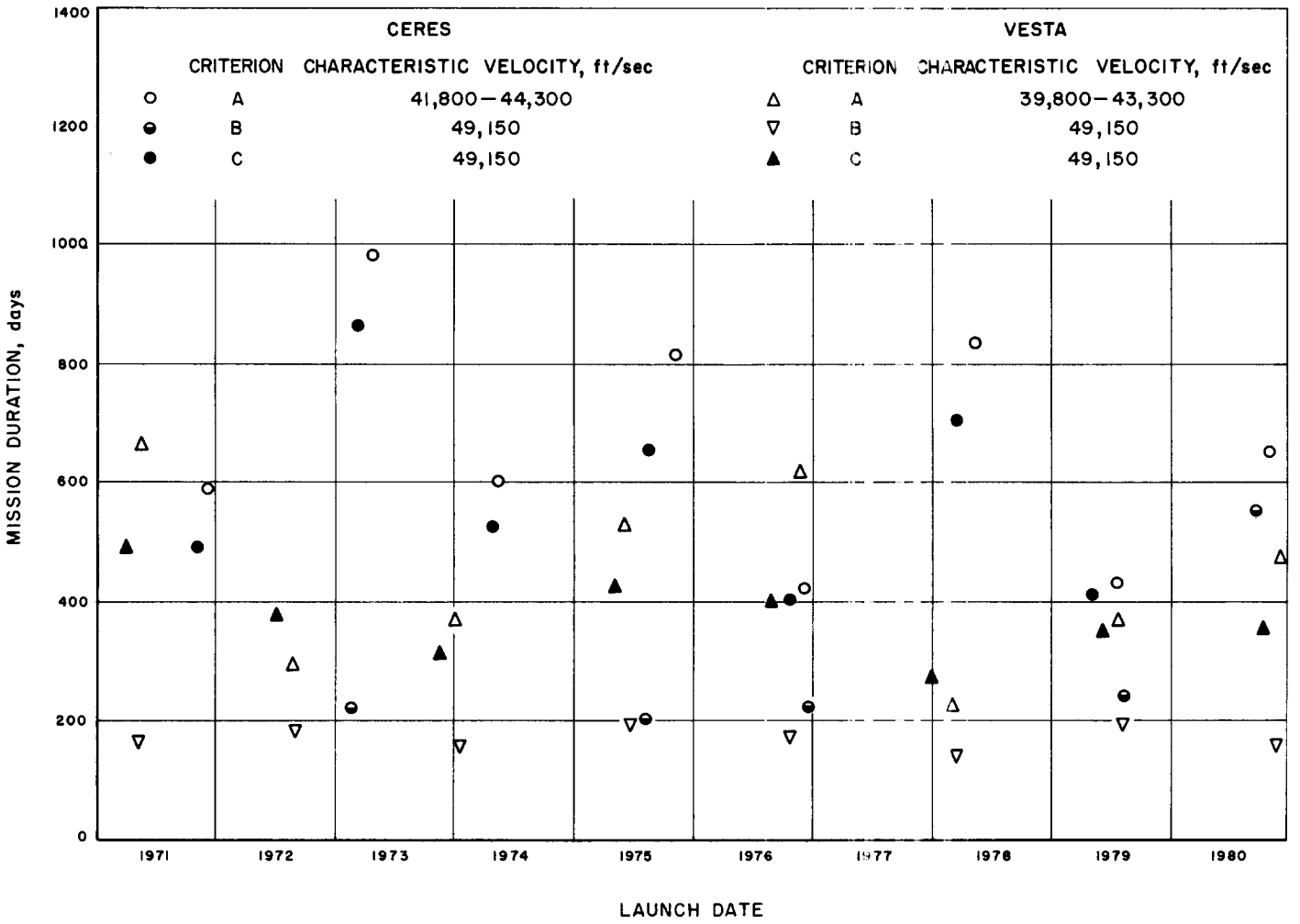

Fig. 1. Minimum trip times for Ceres and Vesta missions (30-day launch window)

from micrometeoroid damage. The latter problem represents a major uncertainty area encountered in the study. The probability of puncture depends on the actual particle distribution encountered. Possible distributions were analyzed and design applications reviewed. A reasonably conservative structural factor of 1.7 lb/ft^2 was used in the design study.

Spacecraft concepts developed for the maximum missions showed much similarity; consequently a universal space bus approach is quite feasible. This concept uses one basic configuration with allowance for "plugging in" of components peculiar to each mission. Thus growth development to a Jupiter flyby is comparatively simple.

A novel feature of the designs employing a large diameter (7 ft) parabolic high-gain antenna is the adopted packaging technique. The antenna is of flex-rib construction and is stowed in a furled condition. After shroud separation, the antenna is swung out, unfurled and orientated towards Earth.

d. Subsystem restraints. Major requirements for mission success arise in the areas of guidance and control, data handling, communications, and power. Fulfillment of these requirements reflects as a weight penalty in the spacecraft. Principal effort was devoted to maximum mission requirements which are the most stringent, but simplification of the subsystems and alternate concepts to achieve the requirements of minimum missions were also studied.

A range of typical science payloads was selected for the design study. These are summarized in Tables 2 and 9 and range from 6 lb (minimum asteroid flyby) to 150 lb (Jupiter flyby). Interplanetary instrumentation is included in the maximum mission packages in addition

[redacted] UNCLASSIFIED

Table 4. Characteristics of Ceres missions (30-day launch window)[a]

Mission date	Nominal departure date (Julian date-2440000 calendar date)			Characteristic velocity, ft/sec			Range of flight times, days			Extremes in communication distance, AU			Maximum departure declination (absolute value), deg			Passage speed variation, ft/sec			Maximum arrival declination (absolute value), deg			Total time spent within 20 Ceres radii (min)[c]			Payload for minimum energy missions, lb			
																									Launch vehicle			
	A	B	C	A	B	C	A	B	C	A	B	C	A	B	C	A	B	C	A	B	C	A	B	C	1	2	3	4, 5
1970	0770	0790	0740	42300	49150	49150	350	220	360	3.65	2.39	3.25	≤28.5	≤28.5	34	25000	42100	22300	20	10	27	32.7	19.4	36.7	2160	1420	0	0
	July 3	July 23	June 3	43200			360	230	370	3.70	2.61	3.58				26000	50400	30300				31.4	16.3	27.0				
1971	1290	X[b]	1230	42000	X		590	X	490	1.77	X	2.45		X	42	23400	X	24200	24	X	38	35.0	X	33.8	2260	1510	0	
	Dec. 5		Oct. 6	42800			690		520	2.09		2.83				23500		27300				34.7		30.0				
1973	1800	1740	1760	43800	49150		980	220	830	1.80	3.13	2.09		41	≤28.5	29800	43500	26100	19	14	29	27.4	18.8	31.3	1900	1240	0	
	April 28	Feb. 27	Mar. 19	44300			1010	250	860	2.43	3.49	2.45				31000	50000	29400				26.4	16.4	27.8				
1974	2190	X	2150	42100	X		600	X	520	1.87	X	2.19		X	38	18800	X	20500	27	X	40	43.5	X	39.9	2060	1360	0	
	May 21		April 13	43600			710		540	2.18		2.46				20600		24600				39.7		33.3				
1975	2720	2660	2660	42800	49150		810	200	650	3.08	2.69	2.26		33	33	31900	51400	28800	18	10	27	25.6	15.9	28.4	2100	1370	0	
	Nov. 4	Sept. 5	Sept. 5	43500			840	210	680	3.59	3.03	2.67				32000	58000	31300				25.5	14.1	26.1				
1976	3130	3140	3090	41800	49150		420	220	400	3.14	2.95	2.72		36	49	18300	28600	21500	28	10	39	44.7	28.6	38.0	2310	1550	260	
	Dec. 18	Dec. 28	Nov. 8	42600			450	240	420	3.20	3.18	3.06				18400	41000	25900				44.4	20.0	31.6				
1978	3630	X	3590	43100	X		830	X	700	2.85	X	3.33		X	33	26400	X	23800	22	X	35	31.0	X	34.4	2070	1360	0	
	May 2		Mar. 23	43600			850		720	3.50		3.52				27400		26600				29.8		30.8				
1979	4050	4060	4000	41900	49150		430	240	410	2.97	3.43	3.33		32	49	19000	41000	21900	26	6	38	43.0	20.0	37.3	2350	1570	300	
	June 26	July 6	May 7	42500			460	270	430	3.04	3.66	3.64				20000	47000	28400				40.9	17.4	28.8				
1980	4650	X	4510	42300	X		650	X	550	1.72	X	1.74		X	38	26500	X	25000	21	X	34	30.9	X	32.7	2100	1370	0	
	Nov. 17		Sept. 28	43500			680		570	2.09		1.88				26700		28300				30.6		28.9				

[a] Mission criteria: A. Minimum energy.

B. Minimum flight time, based on maximum characteristic velocity of launch vehicle No. 1 with 1000-lb payload. Heliocentric travel angles < 180 deg, high-arrival velocities.

C. Intermediate flight time, based on the same as B, but with heliocentric travel angles > 180 deg, low arrival velocities.

[b] Not possible to achieve 30-day launch window.

[c] Pericenter distance of 1000 km.

UNCLASSIFIED

UNCLASSIFIED

Table 5. Characteristics of Vesta missions (30-day launch window)[a]

Mission date	Nominal departure date (Julian date-2440000 calendar date)			Characteristic velocity, ft/sec			Range of flight times, days			Extremes in communication distance, AU			Maximum departure declination (absolute value, deg)			Passage speed variation, ft/sec			Maximum arrival declination (absolute value, deg)			Total time spent within 20 Vesta radii, (min)[b]		
	A	B	C	A	B	C	A	B	C	A	B	C	A	B	C	A	B	C	A	B	C	A	B	C
1969	0560	0540	0480	40400	49150	49150	520	170	380	1.31	2.06	3.15	≤28.5	43	41	25400	40000	20600	20	7	36	16.4	10.4	20.3
	Dec. 5	Nov. 15	Sept. 16	40800			550	180	390	1.90	2.69	3.19				27600	56500	23200				15.1	7.4	18.0
1971	1100	1080	1040	42100			660	160	490	2.53	1.73	2.22	≤28.5	42	38	21500	38600	18600	20	10	36	19.4	10.8	22.5
	May 29	May 9	Mar. 30	42700			700	170	510	3.26	2.18	2.76				22000	48800	21300				19.0	8.6	19.6
1972	1550	1560	1500	42100			290	180	300	3.39	2.45	3.12	38	≤28.5	≤28.5	26400	43500	17100	18	8	15	15.8	9.6	24.4
	Aug. 21	Aug. 31	July 2	43300			310	200	380	3.43	2.90	3.50				27600	56200	31200				15.1	7.5	13.4
1974	2050	2060	1990	39800			370	150	310	3.14	1.68	2.60	≤28.5	≤28.5	47	18900	55000	23900	23	2	34	22.1	7.6	17.5
	Jan. 3	Jan. 13	Nov. 4[c]	40300			390	160	330	3.15	1.79	2.76				19300	56500	27800				21.6	7.4	15.0
1975	2580	2590	2530	41500			530	190	430	1.60	2.42	2.95	≤28.5	34	48	15600	36200	18600	25	6	44	26.8	11.5	22.4
	June 17	June 27	April 28	42300			540	210	460	1.92	2.81	3.46				16100	42400	21300				26.0	9.9	19.7
1976	3100	3070	3000	41100			620	170	400	1.27	2.28	3.16	≤28.5	37	33	29400	56800	17000	16	8	30	14.2	7.4	24.6
	Nov. 18	Oct. 19	Aug. 10	41300			650	190	430	2.01	2.50	3.32				32200	58600	19100				13.0	7.1	21.9
1978	3570	3590	3510	41600			230	140	270	2.64	1.42	2.13	40	≤28.5	≤28.5	23600	49500	17100	20	8	19	17.7	8.4	24.4
	Mar. 3	Mar. 23	Jan. 2	42400			240	150	400	2.31	1.66	3.12				27800	55200	25300				15.0	7.6	16.5
1979	4070	4090	4030	41000			370	190	350	3.38	2.56	3.50	≤28.5	≤28.5	57	15000	35200	21400	15	8	38	27.9	11.9	19.5
	July 16	Aug. 5	June 6	42900			390	210	380	3.56	3.19	3.57				18800	49400	24800				22.2	8.5	16.8
1980	4580	4570	4510	40100			480	160	360	2.07	1.93	3.02	≤28.5	42	43	23500	46000	23800	21	7	37	17.8	9.1	17.6
	Dec. 7	Nov. 27	Sept. 28	40600			490	180	370	2.53	2.23	3.14				24400	56600	24200				17.1	7.4	17.3

[a] Mission criteria: A. Minimum energy.
B. Minimum flight time, based on maximum characteristic velocity of launch vehicle No. 1 with 1000-lb payload. Heliocentric travel angle < 180 deg, high arrival velocities.
C. Intermediate flight time, based on the same as B, but with heliocentric angles > 180 deg, low arrival velocities.

[b] Pericenter distance of 1000 km.

[c] 1973.

Table 6. Subsystem weight and power summaries for alternate system concepts (particle distribution missions)

Subsystem	Mission					
	A1		A2		A3	
	Weight, lb	Average raw power, w	Weight, lb	Average raw power, w	Weight, lb	Average raw power, w
High-gain antenna	5		26		26	
Omniantenna	1		1		1	
Radio (Transmitter operating)	50.4	82	40.4	48	50.4	80
Command decorder and CC&S	25.9	15	25.9	15	25.9	15
Data encoder	8.0	6	8.0	6	31.2	13
DAS	6.0	2.5	6.0	2.5	19.1	8
Inertial reference unit	—	—	15.0	25	30	25
Star trackers	—	—	20.0	8	20	8
Sun sensors	—	—	3.0	1	3	1
Sun gates	4.0	1.5	—	—	—	—
G&C electronic unit	—	—	14.5	20	29	20
Attitude-control (gas, tanks, and nozzles)	—	—	21	5	186	5
Instrumentation	18.0	1.8	19.0	5.9	65	17.6
Spin mechanism	15.0	—	—	—	—	—
Thermal control	12.0	1	15.0	1	21	1
Totals	145.3	109.8	214.8	137.4	507.6	193.6

Table 7. Subsystem weight and power summaries for alternate system concepts (major asteroid flyby missions)

Subsystem	Mission C1		Mission C2	
	Weight, lb	Average raw power, w	Weight, lb	Average raw power, w
High-gain antenna	26		26	
Omniantenna	1		1	
Radio (transmitter operating)	40.4	48	50.4	80
Command decoder and CC&S	25.9	15	25.9	15
Data encoder	8	6	31.2	13
DAS	6	2.5	19.1	8
Tape recorder	19.8[a]	30	41	35
Inertial reference unit	15.0	25	30	25
Scan subsystem	13.1	12	13.1	12
Star trackers	20	8	20	8
Sun sensor	3	1	3	1
Velocity meter	5	7	5	7
G&C electronic unit	14.5	20	29	20
Attitude-control (gas, tanks and nozzles)	21	5	102	5
Instrumentation	6	15	75	50.6
Thermal control	15	1	21	1
Propulsion	46	4	46	4
Total	285.7	199.5	538.7	284.6

[a] 5×10^9 bit capacity, power quoted is for recording; playback at 3 w.

Table 8. Total system weight summaries

Subsystem	Mission						
	A1	A3	B3	C1	C2	Jupiter Flyby	*Mariner* C
Structure	75	203	203	130	193	205	70
Communications and data handling	96	195	195	140	249	236	151
Guidance and control	19	268	268	79	189	273	76
Power	126	233	233	189	314	314	155
Thermal control	12	21	21	15	21	21	15
Propulsion	—	—	—	46	46	36	40
Science[a]	18	129	177	6	128	204	63
Total, lb	346	1,049	1,097	605	1,140	1,289	570

[a] Includes mounting structure and protective covers.

Table 9. Summary of typical scientific packages for maximum missions

Selected instruments	Particle distribution	Particle composition	Major asteroid[a]	Combined particle distribution and composition	Jupiter flyby	
					A	B
Fixed mount						
Ion chamber	1.4	1.4	1.4	1.4	1.4	1.4
Particle flux meter	2.6	2.6	2.6	2.6	2.6	2.6
High-energy proton detector					4	4
Medium-energy proton detector					3	3
Trapped radiation analyzer					4	4
Low energy plasma analyzer	7	7	7	7	7	7
X-Ray detector						5
Magnetometer (helium)	5	5	5	5	5	5
Magnetometer (flux gate)					2	2
Micrometeoroid momentum gage						
High sensitivity	3	3	3	3	3	3
Low sensitivity	6	6	6	6	6	6
Radio noise receiver						3
Bistatic radar			5			
Top-side sounder						25
Movable mount						
Visual TV (low resolution)			6		6	
Visual TV (high resolution)			30		30	
Infrared TV (low resolution)					10	
Photometer/polarimeter			6		6	6
Visual spectrometer						22
IR radiometer			3		3	3
IR spectrometer					29	29
Microwave radiometer					18	18
Multiple film meteoroid monitor	30			30		
Optical meteoroid detector	10			10		
Impact mass/flash spectrometer		2 × 40		40		
Total weight, lb	65	105	75	105	140	149

[a] Requires optical planet tracker to direct instrument platform.

to the basic experimentation. The types of observations planned and the data-acquisition rates anticipated vary for each package and thus govern the remaining subsystem design requirements.

The guidance analyses showed that DSIF tracking is adequate for the accomplishment of all missions. Flythrough missions can be performed with a reasonable guidance accuracy at injection only, since the actual space trajectory followed is not critical. The most stringent requirements arise in a flyby of a major asteroid, as a miss distance of about 100 km is desirable for the performance of scientific observations. Two midcourse maneuvers are required in this case. An examination of the major miss distances attainable at Ceres and Vesta showed (Fig. 2) a sizable variation for the opportunities examined. Only trends can be deduced from this study, but it appears that minimum values of major miss are achieved on missions of short duration (< 300 days). A maximum value is then approached between 400 and 500 days, and lower values are again obtained at longer flight times. No definite relationship to minimum energy missions was discernible, and the conditions relating to each opportunity must be analyzed separately. The important implication is that the accuracy of the miss distance attainable at the target with two midcourse propulsive maneuvers can influence the choice of mission. Similar arguments apply to the Jupiter mission where only one corrective maneuver is required, but, because the miss distance requirements are less stringent ($\sim$10,000 km), the effects are not so important.

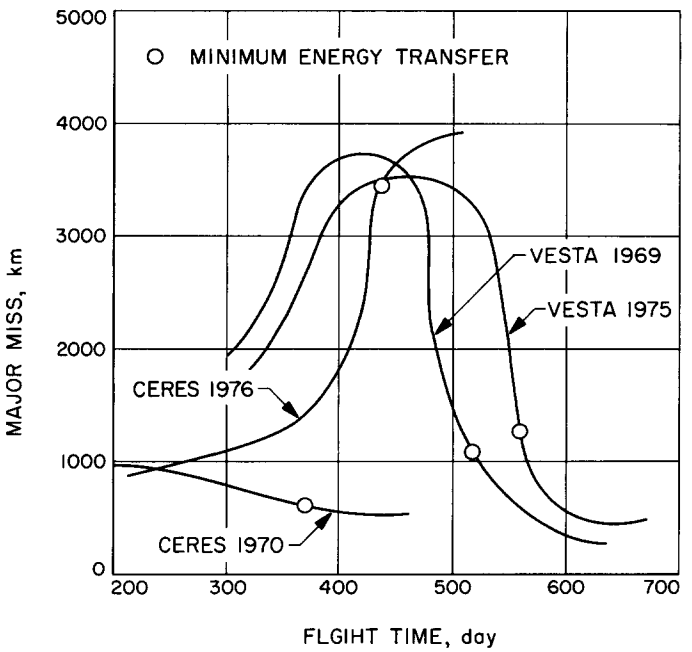

Fig. 2. Guidance accuracy for asteroid flyby missions

Various concepts for attitude control were suggested, and an all-axis stabilization system using the Sun and Canopus as primary references and N_2 gas for propulsion was used for the maximum mission systems. The main weight penalty arises from the fuel required for the proposed reaction system, particularly a redundancy required for reliability. A gyro-inertial unit is required for maneuvers and is used during Jupiter encounter, when the primary references are likely to be obscured.

Spin stabilization (at 50 rpm) of the spacecraft is suggested for the minimum flythrough mission. Spin is imparted at injection from the final launch stage, and a spin axis perpendicular to the plane of the ecliptic is recommended to facilitate communications and data gathering. Scientific objectives of the minimum asteroid flyby mission are achieved at encounter so that no stabilization is required over the cruise phase, except for maneuvers. Therefore, intermittent all-axis stabilization over critical phases of the mission only is suggested.

Table 10. Communication subsystem weight and power summary (maximum missions)

Component	Weight, lb	Average raw power requirements, w	*Mariner C* reference number
High-gain antenna	26	—	
Low-gain antenna	1	—	
Power monitor	0.25	—	2 DC 1
Power monitor and test coupler	0.50	—	2 DC 2
Power Amplifier 1 Power Amplifier 2	10.5	56.0	2 RA 1 2 PS 1 2 CC 1
Exciter 1 Exciter 2	6.0	12.6	2 TR 2
Receiver and transmitter	10.5	11.5	2 RA 1/2 2 TR 1
Chassis and cables	22.65		
Total	77.4	80.1	

The communications subsystem is required to provide a command link and to transmit data from the spacecraft to Earth at a sensible rate and at an acceptable bit-error rate. For maximum missions, where the spacecraft is Sun oriented, a 3.5-db omniantenna with the gain pattern in the general direction of Earth can be used. This antenna provides a command link of 2 bits/sec at a range of 6 AU. Transmission of scientific data on these missions is accomplished by a directional 7-ft parabolic antenna operating at 10 w, which provides a capability of 20 bits/sec at the maximum range associated with the Jupiter mission (6.2 AU). A similar system but operating at 2.5 w satisfies the requirements of missions where intermittent all-axis stabilization is used (Missions A2 and C1). Tradeoffs available between antenna size, operating power and bit rate are given in Table 10. A simple discone antenna is suggested for use on the spinning spacecraft for minimum flythrough missions. Operation at 20 w provides a 1 bit/sec capability at a range of 3.5 AU. No mission restraints are imposed by interference effects arising from the Earth-spacecraft-Sun geometry.

The level at which data can be transmitted has important repercussions in the design of the data-handling system. For the flyby missions, data-storage during encounter is mandatory because of the high acquisition rates resulting from TV observations. Storage during the flythrough missions is also proposed, but for a different reason, viz., data accumulation rates are low, and it is more efficient to store the data in a simple core. The main hope for weight reduction in this area is for an advancement in the state-of-the-art regarding lightweight tape recorders and data compression techniques. The maximum flyby missions result in the greatest accumulated amounts of data, approximately 150×10^6 bits. On the minimum flyby of a major asteroid this value is reduced to 5×10^6 bits because only low-resolution TV is involved. The reduced data rates associated with the minimum missions result in much reduced weight in the required data-handling subsystems.

Although the Asteroid Belt and Jupiter flyby missions all involve trajectories that carry the spacecraft to great distances from the Sun, thermal control does not appear

Table 11. Summary of power profiles for simplified concepts

Mission	Mission phase	Stabilization mode	Subsystem operating	Time	Raw power level, w
A1	Cruise	Spin	All, transmitter at standby	Continuous	73.2
	Data transmission	Spin	All, radio transmitter operating	4 hr/day	109.2
A2	Cruise	No stabilization	Command decoder, CC&S, radio with transmitter at standby, thermal	Continuous	32
	Stabilization maneuver	—	As above plus inertial unit, trackers, attitude-control jets	4 hr 1 per month	92
	Data acquisition and transmission	All-axis	All except inertial unit	24 hr 1 per month	112.7
C1	Cruise	No stabilization	Command decoder, CC&S, radio with transmitter at standby, thermal	Continuous	32
	Stabilization maneuver	—	As above plus inertial unit, trackers, control jets	Near-Earth Near target (4 hr)	92
	Tracking	All-axis	As above, transmitter on, inertial unit off	Near-Earth (5 days) Encounter—20 days (5 days)	98
	Midcourse correction	Inertial	As stabilization maneuver plus transmitter on	Near-Earth Near target (4 hr)	134
	Approach	All-axis	As tracking plus scan subsystem	15 days	110
	Encounter	All-axis	All subsystems except inertial unit	4 hr	163.5
	Playback	All-axis	As above, no instruments or scan	7 days	109.5

to be critical. A minimum weight system is envisaged that employs passive control through the use of suitable surface finishes and insulation deployed at critical areas. The technique depends on the properties of a mosaic surface where the solar absorptance can be fixed at a low value to combat the variation in solar constant throughout the missions, and a suitable value of emittance at the longer thermal wavelengths selected. A reasonable choice of mosaic gives a sensible operating temperature at the target and a value near Earth that is not excessive.

Evaluation of midcourse propulsion unit requirements showed little weight advantages of any of the systems studied and a monopropellant hydrazine system is suggested because of its innate reliability. A cold gas N_2 system is recommended for attitude control, but a concept using a subliming solid appears very attractive for maximum missions due to a weight saving of about 50%. Further work on such a system should prove well worthwhile. For reliability in this critical subsystem, three times the nominal fuel required for the mission is carried on board the spacecraft, as in the *Mariner C* vehicle.

Mission power requirements are summarized in Table 11 for minimum missions and Tables 12 through 15 for maximum missions. These requirements are best met by the use of radioisotope thermoelectric generators (RTG's) with an auxiliary conventional battery. The RTG supply has a number of advantages over one using solar panels. Because of the long ranges from the Sun that are involved, large panel areas would be required, resulting in high weight in comparison with the RTG's. Further, the RTG is less susceptible to meteoroid damage, and its output is independent of the value of the local solar constant. A big disadvantage, however, is the cost and availability. Although SNAP 9A units are presently under test in space vehicles, the problem of a ready supply of isotope fuel could be critical. However, by the 1970's this problem should be eased considerably.

e. Reliability considerations. The approach taken in the reliability analysis was based on the fact that accurate predictions cannot be expected from a detailed component-level study. Thus a broader analysis was developed using Active Element Groups to identify critical areas and illustrate the degree of improvement

Table 12. Asteroid Belt and Jupiter flyby missions common equipment power requirements

Assembly (2400-cycle power)	Reference number*	Peak watts	Lift-off	Average power requirements, w					
				Launch	Acquisition	Cruise	Maneuver	Encounter	Playback
Main inverter	4A15								
DAS	20A5	8.00		2.10	2.10	4.30	2.10	4.30	2.10
Data encoder power supply	6A13	8.00	8.00	8.00	8.00	8.00	8.00	8.00	8.00
Command decoder	3A7	3.79	3.35	3.35	3.35	3.35	3.35	3.35	3.35
CC&S transformer-rectifier	5A8	6.50	6.50	6.50	6.50	6.50	6.50	6.50	6.50
Control system electronics	7A1	10.60			5.70	5.70	5.70	5.70	5.70
Pyrotechnic control	8A1/2	4.00	1.10	1.10	1.10	1.10	1.10	1.10	1.10
Power synchronizer	4A12	1.20	1.20	1.20	1.20	1.20	1.20	1.20	1.20
Receiver transformer-rectifier	2TR1	6.90	6.90	6.90	6.90	6.90	6.90	6.90	6.90
Control unit	2CC1	1.50	0.85	0.85	0.85	0.85	0.85	0.85	0.85
Exciter transformer-rectifier	2TR2	8.00	8.00	8.00	8.00	8.00	8.00	8.00	8.00
Power distribution	4A11	4.00	1.50	1.50	1.50	1.50	1.50	1.50	1.50
Total		62.49	37.40	39.50	45.20	47.40	45.20	47.40	45.20
Maneuver inverter	4A16								
Control system electronics	7A1	42.50					18.5		
Control gyros and electronics	7A2	20.0	6.7	6.7	6.7		15.3		
Total		124.99	44.10	46.20	51.90	47.40	79.00	47.40	45.20

* Reference number corresponds to *Mariner C* subsystem identification used in "Functional Specification Spacecraft Components Design Parameters," Specification Number MC-4-120A, April 18, 1963.

Table 13. Asteroid Belt flythrough power requirements

	Reference number	Peak power	Average power requirements, w					
			Lift-off	Launch	Acquisition	Cruise	Playback	
2400-cycle inverter power	4A15/16							
Common equipment power		124.99	44.10	46.20	51.90	47.40	45.20	
Instrumentation		17.50		7.50	7.50	17.50*	17.50	
Total 2400-cycle power		142.49	44.10	53.70	59.40	64.90	62.70	
Total power input		167.0	51.9	63.2	70.00	76.3	73.8	Efficiency = 0.85
400-cycle 3-phase inverter	4A18							
Control gyros and electronics	7A2	18.0	9.6	9.6	9.6			
Total power input		24.0	12.8	12.8	12.8			Efficiency = 0.75
Regulated DC power	4A8							
Power synchronizer		1.0	1.0	1.0	1.0	1.0	1.0	
Telemetry		2.0	2.0	2.0	2.0	2.0	2.0	
Total DC power		3.0	3.0	3.0	3.0	3.0	3.0	
Total regulator output		194.0	67.7	79.0	85.8	79.3	76.8	
Total regulator input		258.0	90.1	105.1	114.5	105.5	102.3	Efficiency = 0.75
Raw DC power								
Power amplifiers	2 PSI	56.0	15.0	56.0	56.0	20.0	20.0	
Total primary power	(Raw DC)	314.0	105.1	161.1	170.5	125.5	122.3	
Duty cycle or hours		10%	1 hr	1 hr	4 hr	100%	100%	
Primary power required = 150 w Battery capacity = 800 w/hr								
Particle distribution mission shown. Requirement for particle composition mission is 22.0 w.								

over present-day technology that is required. Critical subsystems are guidance and control, communications, and data handling.

An estimate of the mission reliability with state-of-the-art nonredundant subsystems showed that the probability of total mission success is around 2%. This value of course is unacceptable, and it was further shown that to obtain a 90% expectation of success requires a reliability approaching 99% in the various subsystems. The next step was a study of the improvement to be expected by the use of redundancy. The results showed that standby redundancy was preferable to parallel redundancy. The degree of redundancy is limited because of complexity and the influence of other factors such as switching reliability. To indicate solutions of this problem an analysis was made of the improvement in mean operating lifetime required to achieve 99% reliability with various combinations of redundancy. It was found that, for the most critical subsystems, improvement factors of between 5 and 10 are required.

Mission time is the overriding factor influencing mission success. This fact leads one to consider the possibilities of partial success on the various missions. This concept is less meaningful for the flyby missions where the scientific objectives are achieved in the final encounter phase. Thus, the inclusion of instruments to make interplanetary measurements enroute to the target is recommended to increase the chances of partial success. Flythrough missions are more attractive in this context, since important information would be gathered continuously. Unless only one principal experiment is planned for a mission, redundancy of instrumentation is not suggested. Rather, a variety of experiments should be performed to improve the reliability of at least some information being obtained.

A major consideration for improving the probability of partial or total success is an obvious one — the reduction of mission time. Thus, fast trips, taking full advantage of the available launch vehicle capability, are attractive.

Table 14. Major asteroid flyby power requirements

	Reference number	Peak power	Average power requirements, w							
			Lift-off	Launch	Acquisition	Cruise	Maneuver	Encounter	Playback	
2400-cycle inverter power	4A15/16									
Common equipment power		124.99	44.10	46.20	51.90	47.40	79.00	47.40	45.20	
Instrumentation		56.2			7.6	7.6		56.2		
Tape electronics and transformer-rectifier	16A4	5.6						5.6	3.0	
Scan electronics and transformer-rectifier	31A2	3.0						3.0		
Total 2400-cycle power		189.79	44.10	46.20	59.50	55.00	79.00	112.20	48.20	
Total power input		223.0	51.9	54.4	70.1	64.7	93.0	132.2	56.7	Efficiency = 0.85
400-cycle 1-phase inverter	4A17									
Scan electronics and transformer-rectifier	31A2	3.5						3.5		
Tape machine	16A1	10.4						10.4	<0.01	
Total 400 cycle 1-phase power		13.9						13.9		
Total power input		21.4						21.4		Efficiency = 0.65
400-cycle 3-phase inverter	4A18									
Control gyros and electronics	7A2	18.0	9.6	9.6	9.6		9.6			
Total power input		24.0	12.8	12.8	12.8		12.8			Efficiency = 0.75
Regulated DC power	4A18									
Power synchronization and telemetry		3.0	3.0	3.0	3.0	3.0	3.0	3.0	3.0	
Total regulator output		271.4	67.7	70.2	85.9	67.7	108.8	156.6	59.7	
Total regulator input		362.0	90.1	93.6	114.5	90.4	144.9	209.0	79.6	Efficiency = 0.75
Raw DC power										
Power amplifiers	2PSI	56.0	15.0	56.0	56.0	20.0	56.0	35.0	56.0	
Total DC power	(Raw DC)	418.0	105.1	149.6	170.5	110.4	200.9	244.0	135.6	
Duty cycle or hours		10%	1 hr	1 hr	4 hr	100%	4 hr	6 hr	100%	

Primary power required, 150 or 225 w.
Battery capacity, 1200 or 600 w-hr.

Table 15. Jupiter flyby power requirements

	Reference number	Peak power	Average power requirements, w							
			Lift-off	Launch	Acquisition	Cruise	Maneuver	Encounter	Playback	
2400-cycle inverter power	4A15/16									
Common equipment power		124.99	44.10	46.20	51.90	47.40	79.00	47.40	45.20	
Instrumentation		67.8			9.1	9.1		67.8		
Tape electronics and transformer-rectifier	16A4	5.6						5.6	3.00	
Scan electronics and transformer-rectifier	31A2	3.0						3.0		
Total 2400-cycle power		201.39	44.10	46.20	61.0	56.50	79.00	123.8	48.20	
Total power input		251.5	51.9	54.4	71.8	66.5	93.0	144.3	56.70	Efficiency = 0.85
400-cycle 1-phase inverter	4A17									
Scan electronics and transformer-rectifier	31A2	3.5						3.5		
Tape machine	16A1	10.4						10.4	<0.01	
Total 400-cycle 1-phase power		13.9						13.9		
Total power input		21.4						21.4		Efficiency = 0.65
400-cycle 3-phase inverter	4A8									
Control gyros and electronics	7A2	18.0	9.6	9.6	9.6		9.6	9.6		
		24.0	12.8	12.8	12.8		12.8	12.8		Efficiency = 0.75
Regulated DC power	4A8									
Power synchronization and telemetry		3.0	3.0	3.0	3.0	3.0	3 0	3.0	3.0	
Total regulator output		299.9	67.7	70.2	87.6	69.5	108.8	181.5	59.7	
Total regulator input		398.0	90.1	93.6	116.8	92.6	144.9	242.0	79.6	Efficiency = 0.75
Raw DC power										
Power amplifiers	2PSI	56.0	15.0	56.0	56.0	20.0	56.0	15.0	56.0	
Total DC power	(Raw DC)	454.0	105.1	149.6	172.8	112.6	200.9	257.0	135.6	
Duty cycle or hours		10%	1 hr	1 hr	4 hr	100%	4 hr	16 hr	100%	

Primary power required, 225 w.
Battery capacity, 800 w-hr.

UNCLASSIFIED

5. Performance Evaluation and Mission Selection Considerations

The Asteroid Belt flythrough missions are the easiest to assess since the conditions are invariant with launch date. The major factors influencing the mission performance are, therefore: (1) spacecraft weight, (2) velocity of the asteroidal particles relative to the spacecraft, (3) required aphelion of the trajectory, (4) mission duration, and (5) launch vehicle performance.

The two most important factors are spacecraft weight and launch vehicle performance. For the simplest and most readily available boosters, only minimum missions are possible. More tradeoffs are available if the higher performance (3-stage) launch vehicles are considered.

A simple and informative approach to the question of launch vehicle compatibility is to disregard the spacecraft design studies for a moment and discuss only the launch vehicle capability represented by Fig. 3. Reference to Figs. 3(a) and 4 shows that the *Atlas/Centaur* vehicle, which represents the highest performance of the simple 2-stage boosters, is capable of launching a payload of 700 lb on a trajectory with an aphelion at 2 AU. The associated characteristic velocity is 39,200 ft/sec, and on such a mission scientific experiments could be performed only at the extreme edge of the Asteroid Belt. The *Atlas/Agena D* could be used for a similar mission but the payload capability is only 350 lb. A 30% floxing of the *Atlas* vehicle in combination with the *Centaur* improves the payload capability to 1500 lb, but the maximum payload potential drops to 350 lb for a mission with an aphelion at 3 AU. If a high-energy kick stage (HEKS) is added to the unfloxed *Atlas/Centaur*, a 1000-lb payload could be projected to 5.8 AU. The highest performance vehicle used in the study; viz., 30% flox *Atlas/Centaur*/HEKS is capable of launching 1500-lb payloads to any point in the Asteroid Belt.

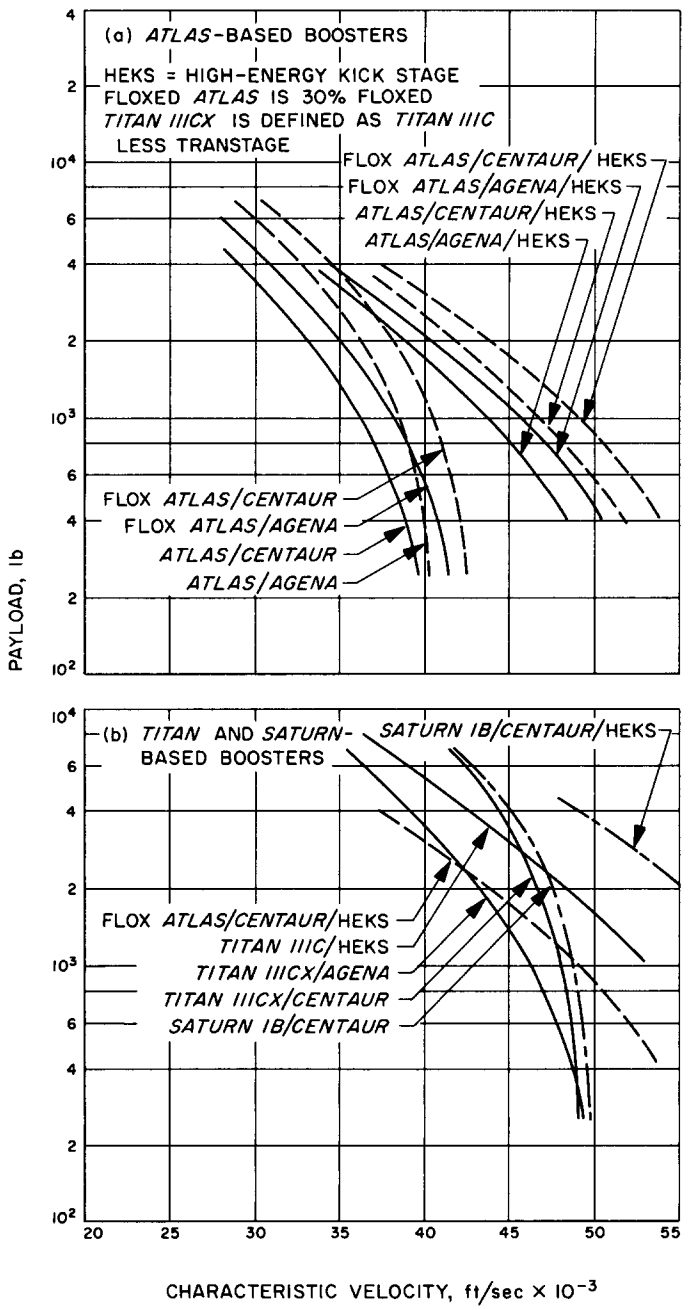

Fig. 3. Typical launch vehicle capabilities (a) *Atlas*-based boosters, (b) *Titan*- and *Saturn*-based boosters

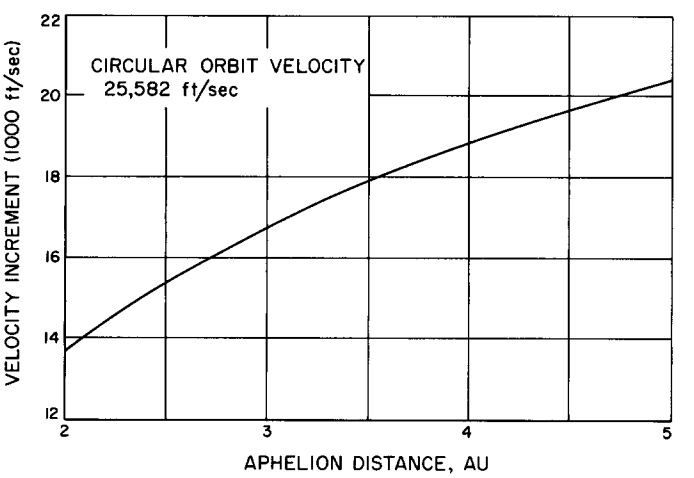

Fig. 4. Velocity increment from 100 nm orbit for asteroid flythrough missions

UNCLASSIFIED

a. Particle distribution mission. The spacecraft weights for this mission range from the minimal value of 346 lb to 1049 lb for maximum missions. Thus a minimum mission to 2 AU could be accomplished with an *Atlas/Agena D* launch vehicle. The use of an *Atlas/Centaur* enables a minimum mission to be performed with an aphelion at 2.25 AU. Both trajectories would just skirt the edge of the inner Asteroid Belt, but would still provide valuable data for the planning of more comprehensive missions. To accomplish maximum missions within the belts a 3-stage vehicle is desirable. Possible missions are summarized in Table 16.

Table 16. Summary of possible Asteroid Belt flythrough missions to measure particle distributions

Launch system	Launch vehicle No.	Possible missions
Atlas/Agena D	5	Minimum mission to 2.0 AU
Atlas/Centaur	6	Minimum mission to 2.25 AU
30% Flox *Atlas/Agena D*	4	Minimum mission to 2.6 AU
30% Flox *Atlas/Centaur*	3	Minimum mission to 3.05 AU Maximum mission to 2.35 AU
Atlas/Agena D/HEKS	11	Any minimum mission Maximum mission to 3.45 AU
Atlas/Centaur/HEKS	12	Maximum mission to 5.25 AU
30% Flox *Atlas/Agena D/HEKS*	2	Maximum mission to 4.6 AU
30% Flox *Atlas/Centaur/HEKS*	1	Any maximum mission

b. Particle composition mission. Since the design payloads are similar and may be regarded as the same within the accuracy of the estimates, the above remarks also apply to the flythrough mission planned for measurement of the composition of asteroidal material.

c. Missions to specific asteroids. Ceres and Vesta are recommended as the most suitable targets. The spacecraft design is the same for each mission and final target choice can be made at quite a late date in the program. Over-all, the Vesta missions are less demanding in energy requirements. Table 17 lists the most attractive opportunities for minimum energy missions to both asteroids, based on velocity requirements and trip time. The values of velocity and trip times quoted are maximum ones for a 30-day launch window.

Table 17. Optimum minimum-energy missions to Ceres and Vesta

Year	Asteroid	Mission duration, days	Characteristic velocity, ft/sec	Criterion
1970	Ceres	360	43,200	Mission duration
1972	Vesta	310	43,300	
1976	Ceres	450	42,600	
1978	Vesta	240	42,400	
1979	Ceres	460	42,500	
1969	Vesta	550	40,800	Velocity requirement
1971	Ceres	690	42,800	
1974	Vesta	390	40,300	
1976	Ceres	450	42,600	
1979	Ceres	460	42,500	
1980	Vesta	490	40,600	

The 1976 mission to Ceres appears to be attractive on both criteria and is similar in velocity requirements to the 1978 Vesta mission, but the latter has the much shorter trip time. It should be noted, however, that the guidance accuracy for the 1976 minimum energy mission to Ceres is not acceptable (miss distance, 3500 km). A due-east launch (Table 5) is impossible for the 1978 Vesta mission, but the departure declination of 40 deg is considered acceptable from range safety considerations.

The spacecraft weight for maximum missions is 1140 lb. This means that the 1974 mission to Vesta is just possible using a 30% flox *Atlas/Centaur* launch vehicle. Reduction of the payload to 1000 lb allows the application of this vehicle to the 1969, 1974 and 1980 missions. All missions through the decade are possible when a HEKS is used with any of the *Atlas*-based boosters. If a minimum mission is contemplated, the 1974 Vesta mission is just feasible with a 30% flox *Atlas/Agena D*. The lowest energy launch system for use on any Ceres mission is the *Atlas/Agena*/HEKS. With this system, the 1971, 1976, and 1979 could be performed with the maximum spacecraft concepts and all minimum mission opportunities could be utilized.

When the important influence of reliability (reflected in trip times) is taken into account, great advantages are obtained from using the highest energy launch vehicle available, since the excess payload capability over the design value can be transformed into increased launch speed. However, if the heliocentric travel angle is less than 180 deg, missions to Ceres with the nominal 1000-lb payload are not possible in 1971, 1974, or 1978 for a 30-day

Table 18. Possible Jupiter flyby (minimum energy) missions

Year	Compatible launch vehicle	Payload, lb
All years	30% Flox *Atlas*/*Centaur*/HEKS	
1971	*Atlas*/*Centaur*/HEKS	1000
1975	*Atlas*/*Centaur*/HEKS	
1970, 1971, 1975, 1980	30% Flox *Atlas*/*Centaur*/HEKS	1300

Table 19. Performance, reliability, schedule and cost factors for mission concepts

Factor	Relevant parameter	Mission			
		Asteroid Belt flythrough (particle distribution)	Asteroid Belt flythrough (particle composition)	Major asteroid flyby	Jupiter flyby
Performance	Payload range, lb	346 to 1097	346 to 1097	605 to 1140	1289
	Characteristic velocity Minimum energy, ft/sec	39,200 for 2AU aphelion 42,800 for 3.2AU aphelion 44,400 for 4AU aphelion		41,800 to 44,300 (Ceres) 39,800 to 43,300 (Vesta)	46,000 to 49,200
	Trip time Minimum energy, days	335 to 2AU 570 to 3.2AU 720 to 4AU		Min: 360 (Ceres) 240 (Vesta) Max: 1010 (Ceres) 700 (Vesta)	Min: 630 Max: 1200 Variation through 30-day launch window ~ 1 yr
Reliability		Improvement in reliability of critical subsystems (guidance and control, communications and data handling) approaching one order of magnitude required for 90% probability of mission success			
	Partial success index[a] Total success index[a]	1 2	1 2	2 1	3 3
Schedule	Go-ahead to launch (yr)	3½	3½	3½	3½
	Long lead items	Development of proposed instrument concepts 1½ yr			
		Design and development of HEKS if required (2½ yr)			
	DSIF requirements Maximum missions Minimum missions	8 min/day 2.5 hr/day	9 min/day 2.5 hr/day	5 min/3 day + 30 days after encounter 7 days after encounter	15 min/2 day + 85 days after encounter —
	Special requirements	Stringent reliability and quality control for all spacecraft and components			
Cost	Program costs for 2 flight articles + 1 standby, excluding launch vehicles (millions of dollars)	48	49	56	52

[a] 1, 2, 3 are qualitative indices only and refer to decreasing chance of success.

launch window. All other missions are possible. As an example, employing a 30% flox *Atlas/Centaur*/HEKS launch vehicle and a 1000-lb payload, trip times of 150 to 200 days are available for Vesta missions at all opportunities if the travel angle is less than 180 deg. If the heliocentric travel angle is greater than 180 deg, trip times are greater, but arrival speeds at the target are reduced. A consideration of the capability of taking TV pictures under the arrival conditions deduced from these two conditions, however, indicate that the target passage time is not critical. Thus, advantage should be taken of the reduced mission durations resulting from trajectories based on a travel angle less than 180 deg. The guidance analysis indicates, also, that short trip times are desirable for giving small miss distances at the target, but further analyses in this area are required before the complete impact of guidance restraints on the missions can be evaluated.

d. Jupiter flyby. The Jupiter missions are characterized by long trip times for minimum energy transfers. Characteristic velocities range from 47,000 to 49,000 ft/sec for a 30-day launch window. Mission durations vary by as much as one year through the window so that actual launch date is important. All missions are considered marginal with the *Atlas*-based launch vehicles. Table 18 summarizes possible missions with two spacecraft weights.

In view of the marginal nature of the missions using the best performance available with *Atlas*-class vehicles and the long trip times involved (~2-yr), it is concluded that some larger launch vehicle, such as one based on *Saturn 1B* or *Titan IIIC*, be considered for the Jupiter mission. As an example, the use of a *Titan IIIC*/HEKS combination would result in payloads approaching 2000 lb for minimum energy. If the payload is set at about 1300 lb, trip times can be reduced to about 500 days with considerably less variation through the launch window. The *Saturn 1B/Centaur*/HEKS would provide even more attractive mission performance. However, in all cases, a kick stage is desirable to provide a high enough Earth departure speed to insure a reasonable trip time.

6. Comparison of System Concepts

Table 19 presents a comparison of the system and mission concepts in terms of performance, reliability, schedule and cost factors. Detailed discussion of these factors can be found at various places throughout the report and only the main points are summarized in the table. Schedule and cost data refer to maximum missions only. Only qualitative data can be given for the reliability estimates since, as explained in the text, detailed analyses would be meaningless at this stage.

B. 1969 Variable-Orbit Mars Atmospheric Probe

1. Introduction

In mid-November 1964, the Office of Advanced Technical Studies initiated a study of a 1969 Mars orbiting capsule mission utilizing an *Atlas/Centaur* launch vehicle.

The purpose of the study was to determine if there existed a mission of significant scientific and/or engineering interest for a Mars capsule orbiter in combination with a flyby bus using a nonfloxed *Atlas/Centaur* vehicle for 1969. Previous study had indicated that no attractive fully-stabilized orbiter mission could be achieved in 1969 with an *Atlas/Centaur* vehicle unless a high degree (30%) of floxing were employed.

Time and manpower limitations did not permit a determination of the technical feasibility of this mission. The objective was, instead, to define a possible mission and determine what objectives might be achieved by an orbiting capsule. Those capabilities which are unique to such a vehicle must be identified and their desirability must be considered. These capabilities should then be compared with what could be accomplished from a flyby vehicle using the full weight capability of the combined mission studied here.

Study results indicate that a unique engineering measurement is the determination of the high altitude (200 to 1,500 km) density profile of the Mars atmosphere. Accurate knowledge of the high altitude density is required to establish the orbit lifetime of a Mars orbiter spacecraft for a given orbit. Conversely, if a minimum orbit lifetime of an (unsterilized) orbiter is specified, the minimum periapsis altitude is determined..

Possible scientific measurements include mapping of the surrounding magnetic field and trapped radiation, photometric observations of the atmosphere and the

surface under various lighting conditions, and determination of the figure of the planet. It is concluded that there are significant unique engineering and scientific measurements which can be accomplished by the Mars orbiter-capsule concept.

2. Summary

A preliminary study of a 1969 Mars capsule orbiter mission has been performed. The most interesting and unique mission examined is a sterilized, variable-orbit atmospheric probe. The high-altitude density is determined by observing the rate of decay of the probe's highly eccentric orbit; this measurement is based on two-way doppler tracking by the DSN. The present uncertainty in the Mars high-altitude atmospheric density appears to place severe limitations on observational capability of planned *Voyager*-class orbiting spacecraft. The initial periapsis altitude for such missions must be kept sufficiently high to guarantee a minimum orbit lifetime of at least 50 yr for an unsterile orbiter. This minimum altitude appears to be 2,000 to 4,000 km, depending on the high-altitude atmospheric model assumed.

In addition to determination of the high-altitude density, other possible in-orbit measurements include mapping of the surrounding magnetic field and trapped radiation (from altitudes of 50,000 km to as low as 200 km), photometric observations of the atmosphere and the surface under various lighting conditions, and determination of the figure of the planet. Approximately 30 lb are available for science instrumentation.

The capsule orbiter is Sun-stabilized and spinning (at 60 rpm) when in orbit. Power is provided by solar cells and a standby battery. A unique conically roll-symmetric antenna provides approximately 12 db of gain toward Earth. This antenna design takes advantage of the fact that the Earth-Mars-Sun angle changes only a few degrees over several months following Mars encounter. With 20 w of radiated power and the use of a 210-ft DSN antenna, a data rate of 8⅓ bits/sec can be maintained for up to 60 and 90 days following the last Type II and Type I arrival dates, respectively.

A pulsed hydrazine system provides attitude-control torques to keep the capsule Sun-oriented; this system also provides torques to permit capsule precession to other attitudes, if desired (e.g., the orbit insertion maneuver). A simple zero-crossing planet detector in combination with a special central capsule sequencer provides synchronizing pulses to establish a third-axis reference prior to the orbit insertion maneuver.

The principal velocity increment to establish a Mars orbit is provided by a solid propellant motor. The lesser velocity increments necessary to reduce periapsis altitude, after the initial orbit is established, are provided by the same pulsed hydrazine system previously described.

The total capsule system weight, including its separation functions and retropropulsion system, is between 750 and 800 lb, depending on the science instrument complement. This weight includes a 15% design margin allowance for the active (in-orbit) capsule orbiter. However, no design margin has been allowed for the propellant.